

Running title: Primary somatosensory cortex connections.

Title: Afferent connections of the primary somatosensory cortex of the mouse for contextual and multisensory processing.

Author: Ian Omer Massé PhD¹, Sohen Blanchet-Godbout², Gilles Bronchti PhD², Denis Boire PhD²

Affiliations:

¹Research Center, Hôpital du Sacré-Cœur de Montréal, 5400 Gouin Ouest Blvd, Montreal, Quebec, Canada, H4J 1C5

²Département d'Anatomie, Université du Québec à Trois-Rivières, 3351, des Forges Blvd, C.P. 500, Trois-Rivières, Quebec, Canada, G9A 2W7

Number of pages:

Number of figures:

Number of tables:

Number of equations:

Total number of words:

Number of words in abstract:

Keywords: Cross-modal, corticocortical connections, subcortical connections, feedforward, feedback, top-down, bottom-up

Corresponding author:

Ian Omer Massé PhD
Centre de recherche
Hôpital du Sacré-Cœur de Montréal
5400, boulevard Gouin Ouest
Montréal, Québec
H4J 1C5

Phone: 514-338-2222 ext 7711

FAX: 514 338-2694

E-mail address: ian.masse.im@gmail.com

Abstract:

Sensory information is conveyed from peripheral receptors through specific thalamic relays to primary areas of the cerebral cortex. Information is then routed to specialized areas for the treatment of specific aspects of the sensory signals and to multisensory associative areas. Information processing in primary sensory cortices is influenced by contextual information from top-down projections of multiple cortical motor and associative areas as well as areas of other sensory modalities and higher order thalamic nuclei. The primary sensory cortices are thus located at the interface of the ascending and descending pathways. The theory of predictive coding implies that the primary areas are the site of comparison between the sensory information expected as a function of the context and the sensory information that comes from the environment. To better understand the anatomical basis of this model of sensory systems we have charted the cortical and subcortical afferent inputs in the ipsilateral and contralateral hemispheres of the primary somatosensory cortex of adult C57Bl/6 mice. Iontophoretic injections of the b-fragment of cholera toxin were performed inside the mystacial caudal barrel field, more rostral barrel field and somatosensory cortex outside the barrel field to test the hypothesis that differences exist between these three parts and to compare their projections to the subnetworks built from the Mouse Connectome Project data. The laminar distribution of retrogradely labeled cell bodies was used to classify the projections as feedback, feedforward or lateral. Layer indices range between -1 and 1, indicating feedback and feedforward connections respectively. The primary somatosensory cortex and the barrel field have afferent connections with somatosensory areas, non-somatosensory primary sensory areas, multisensory, motor, associative, and neuromodulatory areas. The caudal part of the barrel field displays different and more abundant cortical and subcortical connections compared to the rest of the primary somatosensory cortex. Layer indices of cortical projections to the primary somatosensory cortex and the barrel field were mainly negative and very similar for ipsilateral and contralateral projections. These data demonstrate that the primary somatosensory cortex receives sensory and non-sensory information from cortical and subcortical sources.

Introduction

Sensory processing is based on countercurrent feedforward and feedback flow of information and the processing in the primary sensory cortices involves an interaction between these bottom-up thalamocortical and top-down direct corticocortical (Mumford, 1992; Rao and Ballard, 1999; Gilbert and Li, 2013; Zhang et al., 2014; Makino and Komiyama, 2015) and indirect cortico-thalamo-cortical pathways (Sherman and Guillery, 2002; Sherman, 2005; Theyel et al., 2010; Roth et al., 2016).

Recent studies view cortical areas as adaptive processors. Instead of making stereotypical processing of incoming sensory information, different analysis are performed as a function of both sensory and behavioral context. Contextual information is provided to primary sensory cortices by top-down cortical projections and by higher order thalamic nuclei. Moreover, it has been proposed that perception results from a reverberation between feedforward and feedback information and that neurons in early stages of sensory processing are adaptive processors multiplexing between functions as instructed by feedback projections from higher cortical areas (Gilbert and Sigman, 2007; Gilbert and Li, 2013). Top-down modulation by feedback projections to early sensory processing is thought to integrate local and global levels of analysis (Gilbert and Li, 2013; Teufel and Nanay, 2017). Top-down modulation is also provided by non-sensory sources such as attention, expectation and stimulus context (Roelfsema et al., 1998; Ito and Gilbert, 1999; Summerfield and Egner, 2009; McManus et al., 2011; Jiang et al., 2013) and memory (Moore and Cavanagh, 1998). Moreover, conscious perception might depend on top-down inputs from higher order cortices to primary sensory cortices (Meyer, 2011). Indeed, early activity in primary sensory cortices is stimulus-bound whereas later activity

thought to represent top-down incoming information from higher order cortical areas is correlated with conscious perception (Super et al., 2001; Meador et al., 2002; Gutschalk et al., 2008; Hudetz et al., 2009; Meyer, 2011).

Extensive inventories of cortical afferent have been drawn for the primary visual (Charbonneau et al., 2012), auditory (Budinger et al., 2006; Budinger et al., 2008; Budinger and Scheich, 2009) and somatosensory cortices (Zingg et al., 2014) in rodents. In agreement with the wide range of processes that can modulate early sensory processing, these studies have shown a host of top-down cortical projections to primary sensory cortices that comes from diverse motor, association and from cortices devoted to other sensory modalities supporting the position of primary cortices at the interface of ascending and descending pathways.

The laminar distribution of the cortical neurons projecting to primary visual and auditory cortices shows a wide range of structures, some projections arising almost exclusively from infragranular layers whereas other projections arise from all cortical layers (Budinger et al., 2006; Budinger et al., 2008; Budinger and Scheich, 2009; Charbonneau et al., 2012). Ascending and descending cortical projections have different morphological and functional features. Specifically, feedforward connections originate from neurons mainly located in supragranular layers and terminate in the granular layer, whereas feedback connections originate mainly from neurons located in infragranular layers and avoid the granular layer (Rockland and Pandya, 1979; Felleman and Van Essen, 1991). Lateral connections originate equally from infragranular and supragranular layers. A similar hierarchical organization of visual cortices based on feedback and feedforward corticocortical connections has been suggested for the rat (Coogan and Burkhalter, 1990;

1993; Sieben et al., 2013) and mouse (Godement et al., 1979; Yamashita et al., 2003; Dong et al., 2004; Berezovskii et al., 2011). In rodents however, feedforward projections terminate in all cortical layers, not only in granular layer 4 as in primates (Coogan and Burkhalter, 1990).

The somatosensory cortex of the mouse has widespread cortical afferents (Zingg et al., 2014) as those of the visual and auditory cortices. Four somatic sensorimotor subnetworks have been proposed: orofaciopharyngeal, upper limb, lower limb and trunk, and whisker subnetworks, each having specific arrays of cortical connections, along with two medial, and two lateral subnetworks that display unique topologies and can interact through select cortical areas (Zingg et al., 2014). The present study extends this knowledge in providing a quantitative evaluation of afferent cortical and thalamic projections to the primary somatosensory cortex and a laminar distribution of cortical neurons to compare the structure of these corticothalamic top-down connections. Moreover, these features were compared between afferent connections to the mystacial caudal barrel field, more rostral barrel field and somatosensory cortex outside the barrel field to see if the different somatosensory subnetworks follow similar patterns of cortical connectivity.

Material and Methods

Animals and experiment groups

Animals were treated in accordance with the regulations of the Canadian Council for the Protection of Animals and the study was approved by the Comité de bons soins aux animaux de l'Université du Québec à Trois-Rivières. C57Bl/6 mice (n=15) (Charles River, Montréal, QC, Canada) from our colonies were used. All animals were kept under a light/dark cycle of 14/10 hours and were adults (60 days) when sacrificed.

Tracing procedures

Surgical anesthesia was achieved and maintained with inhalation of 1.5-2.5% isoflurane and vital signs were monitored throughout the procedures. The animals were mounted on a stereotaxic apparatus. A scalp incision was made along the midline to expose the skull. For injections in the primary somatosensory cortex outside the barrel field (S1), a small craniotomy was performed 1.5 mm caudal to Bregma and 1.5 mm from the midline or, for injections in the rostral and caudal parts of the barrel field of the primary somatosensory cortex (S1BF), 0.9 mm caudal to Bregma and 2.9 mm from the midline, and 1.5 mm caudal to Bregma and 2.9 mm from the midline respectively. The dura was incised and a glass micropipette (20 μ m tip diameter) filled with 1% solution of the b-fragment of cholera toxin (CTb) (List Biological Laboratories, CA) in phosphate-buffered saline (PBS) was inserted into the cortex into S1 of 5 animals and S1BF of 10 animals. A 1.5 μ A positive current with a 7-s duty cycle was applied for 10 min at depths ranging between 100 and 500 μ m from the pial surface. Starting at a depth of 500 μ m and ending at 100 μ m from the pial surface, 2 min at each 100 μ m. The mice were kept warm

until they recovered from anesthesia. Postoperative pain was managed with buprenorphine (Temgesic, Schering-Plough, Hertfordshire, UK; i.p.; 0.009 mg/kg) injected at the beginning of the procedure.

Perfusion

After a 2-day survival, mice received an intraperitoneal injection of 120 mg/kg sodium pentobarbital (Euthanyl; Bimeda-MTC, Cambridge, ON, Canada) and were perfused through the heart with 0.1 M 0.9% PBS (pH 7.4) followed by phosphate-buffered 4% paraformaldehyde. Brains were harvested, postfixed for 1-2 hours, cryoprotected with 30% sucrose and frozen prior to sectioning for CTb immunohistochemistry processing.

Staining procedures

Serial 50- μ m-thick coronal sections were taken using a freezing microtome. One series was processed for CTb immunohistochemistry and the other series was mounted on slides and stained with cresyl violet to identify the cortical areas of interest and to differentiate the cortical layers. To visualize CTb labeled neurons, free-floating sections were treated for 45 min with 0.15% H₂O₂ and 70% methanol to quench endogenous peroxidase, and thoroughly rinsed in 0.05 M Tris-HCl-buffered 0.9% saline solution (TBS, pH 8.0) containing 0.5% Triton X-100 (TBS-Tx). Sections were then incubated in 2% normal donkey serum (NDS) for 2 hours and transferred to a solution of primary antibody (goat polyclonal anti-CTb 1:4 000; Molecular Probes) with 1% NDS in PBS-Tx for 2 days at 4°C. Subsequently, sections were rinsed in PBS-Tx and incubated in a secondary antibody (biotinylated donkey anti-goat; 1:500; Molecular Probes) solution with 1% NDS in PBS-Tx for 2 hours at room temperature. Following further rinsing, the sections were

then incubated for 90 min in an avidin-biotin complex solution (Elite Vectastain, Vector Laboratories, PK4000 Standard kit) in TBS-Tx, pH 8.0, rinsed in TBS, and then incubated in a 0.015% 3-diaminobenzidine (DBA) solution. Labeled neurons were revealed by the addition of 0.005% H₂O₂. Sections were washed and mounted on gelatin-subbed slides, air-dried, dehydrated and cover-slipped with Permount mounting media (Fisher Scientific, Ottawa, ON, Canada).

Data analysis

All retrogradely labeled neurons found on one of every two sections immunostained for CTb labeling, distributed throughout the whole rostro-caudal extent of the brain, were plotted using an Olympus BX51WI microscope (20 x 0.75 NA objective) equipped with a three-axis computer-controlled stepping motor system (0.05 µm resolution) coupled to a personal computer and to a color Optronix CCD camera and driven by the NeuroLucida software (MBF Biosciences, Williston, VT, USA). In this way, the whole cortex was systematically and randomly sampled on sections 200 µm apart. Cortical and subcortical areas were delineated at lower magnification (4 x 0.16 NA objective) on adjacent Nissl-stained sections. Borders between cortical and subcortical areas were delineated according to the cytoarchitectonic descriptions provided by Caviness (1975) and the mouse brain atlas of Franklin and Paxinos (2008). Contours of each cortical and subcortical area in which retrogradely labeled cells were located were traced with NeuroLucida and the limits of each cortical layer were traced. These contours were superimposed on the images of CTb-reacted sections and resized for shrinkage differences between the Nissl and CTb sections. This allowed plotted neurons in each cortical area to be assigned to supragranular, granular or infragranular layers for the

calculation of layer indices. These indices provide a quantitative assessment of the laminar distribution of retrogradely labeled neurons and are instrumental in the classification of corticocortical feedback, feedforward and lateral connections (Felleman and Van Essen, 1991). Layer indices (L) were calculated using the formula:

$$L = (S - I) / (S + I)$$

where S and I are the number of labeled neurons in supragranular and infragranular layers respectively (Budinger et al., 2006; Budinger et al., 2008; Budinger and Scheich, 2009). The indices range between -1 and 1. Negative values indicate feedback connections mostly originating in infragranular layers and positive values indicate feedforward connections mostly originating in supragranular layers. Values near zero indicate lateral connections. The relationship between the abundance of labeled neurons in the supragranular and infragranular layers of the ipsilateral cortex and the distance for all three injection sites was evaluated by measuring the shortest physical distance between the center of the injection sites and the center of mass of each area.

All photomicrographs were cropped and luminosity and contrast were adjusted with Adobe Photoshop software. Localization of injections sites was illustrated from sections charts extracted from NeuroLucida Explorer software (MBF Biosciences).

Comparison to the Mouse Connectome Project

The afferent cortical projections to S1 from our animals were compared to those reported for S1 injection cases made public on the website of the corticocortical connectivity atlas of the Mouse Connectome Project (MCP, www.MouseConnectome.org) through an interactive visualization tool, the iConnectome. In these cases, double co-injections of

tracers were made into the barrel field and the lower and upper limb region of S1 of 8-week-old male C57Bl/6 mice. Retrograde labeling was achieved through injections of either CTb or Fluorogold. All retrogradely labeled neurons were noted to obtain a qualitative assessment of their presence. A list of our cases and the cases used from the MCP corticocortical connectivity atlas can be found in table 1. Our cases which received injections of CTb outside of the barrel field were compared with the MCP cases which received injections in the upper limb (n=2) and lower limb (n=1) representations of S1, while our cases which received injections inside the rostral part or the caudal part of the barrel field were both compared with the MCP cases which received injections inside the barrel field of the primary somatosensory cortex (n=7).

Antibody characterization

The Anti-Cholera B Subunit antibody (Product # 703, Lists Biological Laboratories) was raised in goat using Cholera B Subunit (Product #104) as the immunogen. The antibody was tested in an immuno-diffusion assay. A 1:4 dilution of the Anti-Cholera B Subunit sera formed an immunoprecipitation during interaction with a 0.5mg/ml solution of Cholera B Subunit (Product #104). The sera showed no reaction in a similar assay against diphtheria toxin (Product #150) or Pertussis Toxin (Product #180).

Statistical analysis

Statistical analyses were performed using SPSS v 16.0 software (SPSS, Chicago, IL, USA). To test for significance of the differences in the relative abundance of labeled neurons, and the layer indices in each cortical area between injection sites, one-way ANOVA and Tukey HSD tests were performed with a significance level of $p < 0.05$.

Results

CTb labeling

Representative CTb injection sites in the somatosensory cortex are illustrated in figure 1A (S1), in the rostral part of the somatosensory barrel field in figure 1B (S1BF) and in the caudal part of the somatosensory barrel field in figure 1C (S1BF). None of the injections involved the underlying white matter. Cases were considered valid only if injections in S1 outside the barrel field retrogradely labeled neurons in the ventral posterior lateral thalamic nucleus (VPL) (Fig. 1D) and if injections in the rostral and caudal parts of S1BF, retrogradely labeled neurons in the ventral posterior medial nucleus (VPM) (Figs. 1E and 1F). CTb injections in S1 and S1BF retrogradely labeled numerous neuronal cell bodies in cortical and subcortical structures in all cases for all the three animal groups. CTb-labeled neurons in the cortex after an injection into the caudal part of the barrel field of S1 are represented in figure 2. All the observed telencephalic and thalamic afferent connections of S1 are represented in figure 3.

Cortical projections to S1

Following injections in S1, many labeled neurons were observed within the somatosensory cortex surrounding the injection sites. These local intra-areal projections were not included in our connectivity charts and were not quantified. In addition, many retrogradely labeled neurons were found in the ipsilateral primary (M1) and secondary (M2) motor cortices and in the secondary somatosensory cortex (S2). Neurons were also found in cortices dedicated to other sensory modalities such as the primary auditory (Au), and in the olfactory piriform (Pir) cortex. Neurons were also observed in association

cortices such as the parietal (PtA) and temporal association (TeA), ectorhinal (Ect), perirhinal (PRh), orbital (OC) and insular (IC) cortices. Labeled neurons were also found in retrosplenial granular and dysgranular (RSG and RSD respectively), prelimbic (PrL), infralimbic (IL), dorsal peduncular (DP) and cingulate (Cg) cortices and in the dentate gyrus (DG) but because of the very low number of labeled neurons and inconsistent occurrence of labeled neurons between our cases, these areas were not included in the statistical analysis. The same ipsilateral cortical projections were observed following injections in the rostral somatosensory barrel field. However, injections in the more caudal aspect of the barrel field produced retrograde labeling of neurons in the primary visual (V1) cortex and in the medial and lateral extrastriate visual areas (V2M and V2L). Injections in S1, and the rostral and caudal parts of the barrel field produced retrogradely labeled neurones in the claustrum.

Callosal projections to the somatosensory cortex were more restricted than ipsilateral projections (Fig. 3). Injections in the three parts of the somatosensory cortex labeled homospecific callosal neurons in the somatosensory cortex and neurons in contralateral motor cortices, M1 and M2, secondary somatosensory cortex and auditory cortices and from ectorhinal, perirhinal and orbital cortices.

The relative weight of ipsilateral (Table 2) and contralateral (Table 3) cortical connections to S1 and the rostral; and caudal parts of S1BF were quantified in each experimental case. All the injection sites in the somatosensory cortex labeled many neurons in the ipsilateral motor cortices M1 and M2, in the secondary somatosensory cortex and in other ipsilateral cortical fields. More robust projections arose from the auditory and visual cortices as well as from parietal and temporal association cortices. As

observed in other studies, the percentage of labeled neurons in each cortex was quite variable making strong statistical decisions on group differences less powerful. Several cortices such as RSG, RSD, PrL, IL, DP, Cg and DG comprised less than 1% of the total number of labeled cortical neurons.

The comparison of the relative abundance of labeled neurons in each cortical area between injection sites (Fig. 4) demonstrates that cortical connections common to the three sites of the somatosensory cortex have many different relative weights. The proportion of labeled cortical neurons in the different cortical areas was quite variable between cases, and only quite large differences reached levels of statistical significance. Indeed, the rostral portion of the barrel field had more robust projections from the motor cortices, M1 and M2 than the non-barrel field portion and the caudal barrel field. Only the difference in the proportion of neurons labeled in M2 between S1 and rostral S1BF reached statistical significance (Tukey-HSD, $p = 0.013$). Conversely the projections of S1 with S2 and Au were more robust than the other injection sites but only the difference between the rostral S1BF and S1 reaches statistical significance (Tukey-HSD, S2 $p = 0.006$; Tukey-HSD, Au $p = 0.025$). Only the caudal barrel field received projections from striate and extrastriate visual cortices (Tukey-HSD, V2M $p = 0.019$; Tukey-HSD, V2L $p = 0.006$). Several differences between fields were detected in the lesser projections. The rostral barrel field injections produced less labeled neurons in the association areas PtA and TeA than injections in S1 (Tukey-HSD, PtA $p < 0.001$) and the caudal barrel field (Tukey-HSD, PtA $p = 0.008$; Tukey-HSD, TeA $p = 0.022$). The caudal barrel field injections also produced less labeled neurons in PtA (Tukey-HSD, $p = 0.047$) than injections in S1. Also, the projection from the piriform cortex was more important in the

caudal barrel field than in S1 (Tukey-HSD, $p < 0.001$) and the rostral barrel field (Tukey-HSD, $p < 0.001$). Finally, the rostral barrel field injections produced more labeled neurons in Cl than injections in S1 (Tukey-HSD, $p = 0.048$).

Callosal projections also demonstrate the heterogeneity of the mouse somatosensory cortex. Homospecific callosal connections seem predominant. Indeed, S1 receives a robust projection from its contralateral homolog and much reduced projections from the contralateral rostral (Tukey-HSD, $p < 0.001$) and caudal (Tukey-HSD, $p < 0.001$) barrel field. Similarly, the rostral barrel field injections produced more labeled neurons in the contralateral barrel field than in the non-barrel field somatosensory cortex (Tukey-HSD, $p = 0.001$). Callosal projections from the motor cortices and secondary somatosensory cortex also show differences between injection sites. Moreover, these differences do not mirror the heterogeneities in the ipsilateral projections. The somatosensory cortex outside the barrel field had a more important projection from the contralateral M1 than the rostral and caudal barrel field (Tukey-HSD, $p = 0.010$). Although the rostral barrel field had more important projections from the ipsilateral M2, this somatosensory area received a relatively smaller callosal projection from this area than the other injection sites. This difference however does not reach statistical significance. A similar inverted pattern of callosal projection is seen with S2 that contributes a relatively stronger projection to the contralateral rostral barrel field compared to the other injection sites for which only the difference with S1 was significantly different (Tukey-HSD, $p = 0.019$).

Contrary to ipsilateral projections, the somatosensory cortex received very few heteromodal callosal projections. The projections from the contralateral auditory cortex were very small and in all cases, no labeled neurons were observed in the primary and

extrastriate visual cortices. The callosal projections from the ectorhinal and perirhinal cortices were of similar weight as M1, M2 and S2. There was a significant between S1 and the caudal barrel field for Ect (Tukey-HSD, $p = 0.001$). The other callosal projections were relatively small and did not show significant differences between injection sites. No significant differences in the percentage of labeled neurons were observed in the contralateral hemisphere between the group which received injections in the rostral part of S1BF and the group which received injections in the caudal part of S1BF.

Layer indices were calculated to scale projections in the feedforward and feedback continuum (Table 4 and 5 respectively and figure 5). In all the cases and for the three injection sites, most of the layer indices of ipsilateral projections had negative values. For the injections in S1 the layer indices ranged between -0.28 in M1 and -0.94 in TeA. Injections in the rostral S1BF produced layer indices ranging between -0.06 in PtA and -0.87 in TeA, and the injections in the caudal S1BF between -0.05 in V1 and -0.91 in TeA. They also show heterogeneities between the three injection sites of the mouse somatosensory cortex. Injections sites in the rostral S1BF produced more negative layer indices for the projections from the motor cortices M1 and M2 and from the secondary somatosensory cortex. Only the difference between rostral and caudal S1BF of the projection from M2 (Tukey-HSD, $p = 0.038$), and the difference between S1 and rostral S1BF of the projection from S2 (Tukey-HSD, $p = 0.023$) reached statistical significance. In all the ipsilateral projections, the layer indices of the projections from the temporal cortices Au and TeA were the most negative and of the same magnitude for all three injection sites. This contrasts with the heteromodal connections with the primary visual cortex, V1, and the medial extrastriate visual cortex, V2M, which were close to zero. The

layer index of the projection from the ipsilateral parietal association cortex, PtA to the rostral S1BF is also very close to zero whereas it is more strongly negative for the projection to S1 and caudal S1BF.

The layer indices of the callosal projections were also mostly negative. There is a similar pattern in the layer indices of the callosal projections from primary somatosensory (S1 and S1BF), motor (M1 and M2), and secondary somatosensory (S2) cortices to the rostral S1BF which were more strongly negative than the projections to the other sites. Not all these differences reached statistical significance however. This is most evident for the projections from S1. The layer indices for this projection to S1 and caudal S1BF were either positive or close to zero whereas the projection to the rostral S1BF was less than -0.7. There was a significant difference between S1 and the rostral (Tukey-HSD, $p < 0.001$) and caudal (Tukey-HSD, $p = 0.012$) barrel field, and between the rostral and caudal parts of the barrel field (Tukey-HSD, $p < 0.001$). There was also a significant difference between S1 and the rostral barrel field for the projections from S1BF (Tukey-HSD, $p = 0.003$). The projections from M2 also followed a similar pattern but differences did not reach statistical significance except between the rostral and caudal parts of the barrel field (Tukey-HSD, $p = 0.025$). Layer indices of the projection from M1 to S1 were positive whereas the layer indices of the projections to rostral and caudal S1BF were very similar and significantly different (Tukey-HSD, $p < 0.001$). Layer indices of the projection from S2 to S1 were less negative than layer indices of the projections to rostral (Tukey-HSD, $p = 0.001$) and caudal (Tukey-HSD, $p = 0.006$) S1BF. The layer indices of the quite weak projection from the auditory cortex to all portions of the somatosensory

cortex had very strongly negative values like the other temporal cortical field TeA. There were no visual heteromodal callosal projections to the mouse somatosensory cortices.

To further visualise the relationship between the structure of ipsilateral and callosal projections, the values of layer indices for each projection in each case were plotted in a scatter diagram (Fig. 6). This shows that in most cases both the ipsilateral and contralateral projections have negative layer indices. In all cases the layers indices were positive for the callosal and slightly negative for the ipsilateral projection from M1 to S1. The projection from M2 to the caudal S1BF had highly variable and inconsistent layer indices values for the ipsi- and contralateral projections. In one case both values are strongly negative and in one case, both are strongly positive. Three cases have intermediate values.

There was no clear relationship between the abundance of labeled neurons in the ipsilateral cortex and the distance for all three injection sites (Figs. 7A, 7C and 7E), without obvious differences between the layer indices (Figs. 7B, 7D and 7F). Since the neurons labeled in the somatosensory cortex were not quantified, very few neurons were charted near the injections sites. This could explain the larger number of neurons in a radius around 4000 μm from the injection sites. The primary and secondary motor cortices as well as the secondary somatosensory cortex almost always had the greatest abundance of neurons, regardless of their distance from the injection sites.

Comparison to the Mouse Connectome Project

The afferent cortical projections to S1 from our animals were compared to those reported for S1 injection cases made public on the website of the corticocortical connectivity atlas

of the Mouse Connectome Project (MCP, www.MouseConnectome.org) through an interactive visualization tool, the iConnectome. A list of our cases and the cases used from the MCP corticocortical connectivity atlas can be found in table 1 and all the observed afferent cortical projections to S1 of our cases and the MCP cases are represented in figure 3.

Our cases which received injections of CTb in S1, outside of the barrel field were compared with the MCP cases which received injections in the upper limb and lower limb representations of S1, while our cases which received injections inside the rostral part or the caudal part of the barrel field were both compared with the MCP cases which received injections inside the barrel field of S1. This implies that in figure 3, the checkmarks next to the boxes which represent a brain structure connected to S1BF that was presented in the MCP are compared with both our cases which received injections in the rostral part of S1BF and the caudal part of S1BF.

There is a general agreement between the connections observed in this study and the Mouse Connectome Project (Fig. 3). Following injections in the upper limb and lower limb representations of S1 in the MCP, labeled neurons were found in the ipsilateral primary (M1) and secondary (M2) motor cortices, in the secondary somatosensory (S2), primary auditory (Au), temporal association (TeA), ecto-rhinal (Ect), perirhinal (PRh), orbital (OC) and insular (IC) cortices. These connections were also observed in our cases which received injections in S1, outside of the barrel field. Moreover, the projections from the parietal association (PtA) and piriform (Pir) cortex to S1, outside of the barrel field, were not observed in the MCP cases. However, we did not observe projections from the claustrum (Cl) to this portion of S1 whereas these projections were reported in

the MCP. Callosal projections to the upper limb and lower limb representations of S1 from M1, M2, S2, Au, Ect and OC were charted in the MCP and observed in our material which received injections in S1, outside of the barrel field, along with other projections from IC and Cl which we did not observe in our material. Callosal projections from PRh were not seen in the MCP cases contrarily to our cases.

Following injections in the barrel field of S1 in the MCP cases, labeled neurons were found in the ipsilateral M1, M2, S2, Au, PtA, TeA, Ect, PRh, OC, IC and Cl as well as the primary visual (V1) cortex and in the medial and lateral extrastriate visual areas (V2M and V2L). Callosal projections to the barrel field of S1 from M1, M2, S2, Au, TeA, Ect, PRh, OC, IC and Cl were charted in the MCP. The same ipsilateral and contralateral cortical projections were observed in our cases following injections in the caudal somatosensory barrel field.

The absence of heterospecific visual callosal projections to the caudal barrel field was also found in the mouse connectome database. However, injections in the more rostral aspect of the barrel field did not produce retrograde labeling of neurons in the ipsilateral V1, V2M, V2L and the contralateral Au, OC and Cl as seen in the MCP cases. We observed projections from the ipsilateral and contralateral piriform cortex to both parts of the barrel field which were not seen in the MCP material.

Subcortical projections to S1

Following injections of CTb into S1 and the rostral and caudal parts of S1BF, retrogradely labeled neurons were found in several subcortical structures of all three animal groups (Table 6). The main sources of thalamic inputs to S1 and S1BF were VPL

and VPM respectively, but due to the high density of labeled neurons therein (Fig. 1), these areas were not included in the statistical analysis. Labeled neurons were found mainly in the posterior thalamic nuclear group (Po), the ventrolateral thalamic nucleus (VL), the ventromedial thalamic nucleus (VM), the reuniens thalamic nucleus (Re), the globus pallidus (GP), the zona incerta (ZI), the central medial thalamic nucleus (CM-PC), the hypothalamus (Hyp) and the laterodorsal thalamic nucleus (LD) (Fig. 8). In addition, some labeled neurons were found in several other thalamic nuclei and subcortical structures. Quantification of the labeled cells is detailed in table 6. Statistical analysis was performed for the nine subcortical structures that consistently contained labeled neurons.

Significant differences in the percentage of labeled neurons in Po, VL, GP and ZI were observed between the group which received injections in S1 and the group which received injections in the rostral part of S1BF (Fig. 9). Post-hoc tests revealed that a greater proportion of labeled neurons was found in ZI (Tukey-HSD, $p = 0.025$) of the group which received injections in S1 compared with the group which received injections in the rostral part of S1BF. Also, a greater proportion of labeled neurons was found in Po (Tukey-HSD, $p < 0.001$), VL (Tukey-HSD, $p = 0.039$) and GP (Tukey-HSD, $p = 0.002$) of the group which received injections in the rostral part of S1BF compared with the group which received injections in S1.

Significant differences in the percentage of labeled neurons in Po, GP, ZI and Hyp were observed between the group which received injections in S1 and the group which received injections in the caudal part of S1BF. Post-hoc tests revealed that a greater proportion of labeled neurons was found in Po (Tukey-HSD, $p < 0.001$), GP (Tukey-HSD, $p = 0.002$), ZI (Tukey-HSD, $p = 0.041$) and Hyp (Tukey-HSD, $p = 0.003$) of the

group which received injections in the caudal part of S1BF compared with the group which received injections in S1. No significant differences in the percentage of labeled neurons were observed in the subcortical structures between the group which received injections in the rostral part of S1BF and the group which received injections in the caudal part of S1BF.

In order to assess and compare the multimodality of the different portions of the mouse somatosensory cortex, the relative importance of cortical projections were grouped according to sensory modality, motor and in functional domains such as multisensory areas and modulatory areas (see Fig. 10). This classification was the same as used by Budinger and Scheich (2009) for the sake of comparison between studies. This analysis shows that S1 and the rostral barrel field receive less multisensory input and input from other sensory modalities, than the caudal portion of the somatosensory barrel field. Indeed, both the ipsilateral and callosal cortical inputs of these areas come mainly from somatosensory and motor cortices. The caudal portion of the barrel field receives an important contingent of projections from somatosensory and motor cortices but received a greater proportion of ipsilateral projections from cortices dedicated to other sensory modalities and also from multisensory association cortices. Callosal projections convey less heteromodal and multisensory projections than the ipsilateral cortical projections. A similar pattern was shown for subcortical projections to the somatosensory cortex. Indeed, the non-barrel field received mainly modality specific afferents from the thalamus whereas the barrel field areas received more multisensory thalamic inputs.

Discussion

Summary

The aim of this study was to shed light on the quantitative and/or structural diversity of the top-down connections to S1, and the rostral and caudal parts of S1BF. The present study has shown that these three parts of S1 have afferent connections with somatosensory areas, non-somatosensory primary sensory areas, multisensory, motor, associative, and neuromodulatory areas.

Top-down influences on early sensory cortices contribute to several functions such as perceptual grouping, constancies and shape recognitions but most importantly they provide contextual information from sensory, motor and association areas of the brain (Gilbert and Sigman, 2007; Gilbert and Li, 2013). The diversity of afferent projections to the somatosensory cortex shown here are commensurate with the afferent projections shown for the visual cortex in the mouse (Charbonneau et al., 2012) and the auditory cortex of the gerbil (Budinger et al., 2008). The present results and these previous studies highlight the diversity of top-down influences on primary sensory cortices in rodents. Whether this diversity is also present in primates is not known, emphasizing the need for brain wide connectivity of the cortex in mammals with a more highly developed cerebral cortex.

Connectomes and modules in the somatosensory barrel field vs. non-barrel field

Compared to previous studies (Zakiewicz et al., 2014; Henschke et al., 2015), the present analysis provides more complete and detailed information on cortical and subcortical afferent projections to S1. A connectomics analysis of the mouse cortex has demonstrated

four subnetworks of the somatosensory cortex (Zingg et al., 2014), the orofaciopharyngeal, upper limb, lower limb and trunk, and whisker subnetworks, along with two medial, and two lateral subnetworks that display unique topologies and can interact through select cortical areas. Our study compared the afferent connections between the mystacial caudal barrel field, more rostral barrel field and primary somatosensory cortex, outside of the barrel field, to see if the different somatosensory subnetworks follow similar patterns of cortical connectivity. Our study also further provides a quantitative evaluation of the thalamic and cortical afferents to the somatosensory cortex of the mouse.

Our study demonstrates that there are indeed differences between the afferent connections of the mystacial caudal barrel field, more rostral barrel field and primary somatosensory cortex, outside of the barrel field. Both S1 and the barrel field have afferent connections with somatosensory areas, non-somatosensory primary sensory areas, multisensory, motor, associative, and neuromodulatory areas but the caudal part of the barrel field displays more varied cortical and subcortical connections compared to the rest of S1. Overall, most of the projections to these three regions of S1 in our cases were from the primary (M1) and secondary (M2) motor cortices, and from the secondary somatosensory cortex (S2). This is consistent with the main somatic nodes within the upper limb, lower limb and whisker subnetworks built from the MCP data, which are M1, M2, S1 and S2, and which are all heavily and reciprocally connected. According to the article published from this data, this organization would allow direct interactions between somatosensory and motor areas in the absence of higher order association areas (Zingg et al., 2014). Indeed, in the MCP data, the processes from the more rostral areas of S1 are more

centered on somatosensory and motor information in the somatic sensorimotor network. This pattern would be better suited to enable rapid integration of different sensory modalities for dynamically regulating motor actions. Similarly, the quantitative evaluation of the cortical afferents to the rostral barrel field in our cases suggests that around 75% of the inputs to this part of S1 are dedicated to somatosensory and motor information compared to 50% for the caudal barrel field.

In addition to most of the connections from M1, M2 and S2, all three regions of S1 which received injections of CTb in our cases had projections from the temporal association (TeA), perirhinal (PRh), and entorhinal (Ect) cortices, which were similar for all three regions. The upper limb, lower limb/trunk, and whisker subnetworks built from the MCP data also share connections with TeA, PRh, and Ect which are three major components of the posterolateral temporal subnetwork (Zingg et al., 2014). This subnetwork would be involved in the processing of visual, auditory, somatosensory, and motor information and such connectivity patterns would support the role of TeA, PRh and Ect in perception, object recognition, and contextual memory associated with emotion (Winters et al., 2008; Aggleton et al., 2010).

The projections to the upper limb representation of S1 seen in the MCP data are similar to the projections to the part of S1, outside the barrel field, in our material, which are mainly from somatosensory and motor areas. However, the lower limb/trunk representation of S1 in the MCP data also receives inputs from visual and auditory areas (Zingg et al., 2014). The part of S1, outside the barrel field, which we compared to both the upper limb and lower limb representations of S1 in the MCP data, had a good percentage of inputs from auditory areas but nothing from visual areas. Taken together with our comparison of the

rostral and caudal parts of the barrel field, this would suggest that the processing of visual information in S1 is limited to the caudal part of S1, outside of the barrel field, as well as the caudal part of the barrel field itself.

Indeed, the lower limb/trunk and whisker representations of S1 in the MCP data were reported to be highly connected with the primary visual and auditory cortices to form major components of the first medial subnetwork (Zingg et al., 2014). According to the article published from this data, the first medial subnetwork would mediate transduction of information between these sensory areas and higher order association areas of the neocortex, providing an interface for direct interactions between different sensory modalities through reciprocal connections among the visual and auditory cortices and the lower limb/trunk and whisker representations of S1. The projections to the caudal part of the barrel field in our material support the implication of this area in such a subnetwork and concretize its position at the interface between ascending bottom-up and descending top-down pathways. Our comparison of the projections between the rostral and caudal parts of the barrel field of S1 indeed shows that it is particularly the caudal part that displays different and more abundant cortical and subcortical connections compared to the rest of S1, by targeting more sensory related cortical areas relevant to exploration such as the auditory and visual cortex along the perirhinal and entorhinal cortex which are implicated in sensory integration and gating (Naber et al., 2000; Rodgers et al., 2008). The quantitative evaluation of our data demonstrates that over 50% of the inputs to the caudal barrel field are dedicated to other sensory modalities, including the processing of visual information. This suggests that somatosensory processing in whisker representations of S1 could be directly influenced by other sensory information.

Multimodality of primary sensory cortices

In traditional models of sensory cortex organization, sensory information processing for each modality is initially segregated in modality-specific sensory areas before subsequent integration in higher-order association areas. This organizational scheme has been challenged by the demonstration of multimodal responses in primary sensory cortices (Ghazanfar et al., 2005; Driver and Noesselt, 2008). Indeed, our data and the data taken from the MCP (Zingg et al., 2014) suggest that somatosensory processing in whisker representations of S1 is directly influenced by other sensory information. The caudal part of the barrel field of S1 receives afferents from more sensory related cortical areas dedicated to other modalities compared to the rest of S1, outside of the barrel field and the rostral-most part of the barrel field. Similarly, the barrel field is part of the medial network built from the MCP data (Zingg et al., 2014), which also shares connections with many sensory related cortical areas dedicated to other modalities.

Other studies on corticocortical connectivity in rodents show that the primary visual (Charbonneau et al., 2012), auditory (Budinger and Scheich, 2009) and somatosensory cortex (Zingg et al., 2014) receives direct inputs from primary sensory cortices of other sensory modalities as well as multisensory and associative cortical areas. It appears that 6.57% of the labeled cell bodies providing inputs to V1 come from somatosensory areas and 28.47% of them come from auditory areas. It appears that only 0.5% of the labeled cell bodies providing inputs to A1 come from somatosensory areas and 1.7% of them come from visual areas. Our data indicates that 9.4% of the inputs to the caudal part of the barrel field come from auditory areas and 10.97% of them come from visual areas.

This part of the primary somatosensory cortex appears to be the most multimodal part of the primary somatosensory cortex.

These results suggest that in rodents, the highest input ratio for “non-preferred” modalities is for V1. This suggests that the visual modality in rodents would benefit the most from heteromodal connections and be the most multimodal of the primary sensory cortices. On the other hand, A1 receives only faint inputs from the other primary sensory cortices (Budinger and Scheich, 2009; Henschke et al., 2015). These observations suggest that the mutual influences between the senses are not equivalent in strength. The influence of the auditory areas on the visual cortex would be the stronger one.

Top-down cortical projections and conscious sensory perception in S1

The three parts of S1 receive afferent projections from several associative areas of higher order, such as the parietal and temporal association cortices, agranular and dysgranular retrosplenial cortices, and the ectorhinal, perirhinal, orbital and insular cortices. Moreover, the laminar distribution of labeled neurons suggests that S1 in mice receives feedback-type projections from these areas. These projections have different structures and could also have different functions since the layer indices, although largely negative, were different in degree. These projections could modulate information in S1 (Bullier, 2001), so that bottom-up signals become consciously perceptible (Tononi and Koch, 2008). Indeed, S1 would have a key role in predictive coding, which is the matching process between the sensory information conveyed by the bottom-up signals and the expectations towards the environment generated by the top-down signals (Grossberg, 1980; Llinas and Pare, 1991; Lee and Mumford, 2003).

Top-down influences in cortical circuits are not homogeneous in function. In the visual system top-down influences can sharpen tuning, provide contextual information, modulate plasticity, etc (Gilbert and Sigman, 2007). The present study more specifically emphasises the structural diversity of top-down influences on the somatosensory cortex subfields. The negative layer indices calculated here demonstrate that top-down influences were provided by more neurons in infragranular than supragranular layers. The layer indices observed here range however between values close to 0 and -1, and are therefore not homogeneous. This diversity of size indices of top-down projections to the somatosensory cortex was greater than those to the visual cortex of the mouse (Charbonneau et al., 2012) and in the auditory cortex of the gerbil (Budinger et al., 2008). Only a few layer indices are given for the mouse afferents to the visual cortex but they were mostly quite strongly negative, as for those shown for the gerbil cortical afferents of the auditory cortex.

The most striking differences in layer index values are between the auditory and visual projections to the caudal barrel field. Indeed, the layer index of the auditory cortex is strongly negative whereas that of the visual cortices V1 and V2M were close to 0. Although negative layer indices seem to be most prevalent in cortical afferent projections to somatosensory, visual and auditory cortices in these rodents, the interconnections between them appear quite different. Lateral type projections with layer indices close to 0 were found here for the projections from the visual cortex and this was also the case in the gerbil (Henschke et al., 2015). This contrasts further with the positive layer index reported in the projections from the visual cortex to the auditory cortex of the gerbil (Henschke et al., 2015).

There are significant functional differences between supra- and infragranular cortical connections. Electrophysiological studies have shown that gamma band oscillations are more prevalent in supragranular neurons (Bollimunta et al., 2011; Buffalo et al., 2011; Xing et al., 2012), whereas beta-band oscillations are more important in infragranular neurons (Buffalo et al., 2011; Xing et al., 2012). It has been suggested that feedback cortical projections might promote beta synchronization between cortical areas and that feedforward projections could promote gamma band interareal synchronizations (Markov et al., 2014). Further studies demonstrated that feedforward processing in the visual system increased activity in the gamma band and that feedback processing increased activity in the theta and beta frequencies (van Kerkoerle et al., 2014; Bastos et al., 2015; Michalareas et al., 2016). Moreover there is a significant correlation between anatomically determined indices of neuron distributions in cortical layers, and beta/gamma band activity in feedback and feedforward projections in monkeys (Bastos et al., 2015).

The predominant negative values in the cortical afferent projections to the somatosensory cortex of the mouse shown here suggest that top-down influences act most importantly in the beta range oscillations. However, we can hypothesize that there is a range in the intensity of synchronization in the beta and gamma frequencies exerted by namely visual and auditory cortices upon the caudal barrel field and also coming from the contralateral cortices in which a wider range of layer indices values were found.

We show here that the strength of corticocortical connections of the somatosensory decreases with distance from the injection sites in all three subfields of the somatosensory cortex of the mouse. This demonstrates that the interareal connectivity rules demonstrated

for the monkey cortex (Ercsey-Ravasz et al., 2013) might also apply to mouse. This also suggest that the mouse cortex interareal connections also develops under the same constraint of wire minimization (Mitchison, 1991; Cherniak, 1994; Cherniak et al., 1999; Chklovskii, 2000; Koulakov and Chklovskii, 2001; Chklovskii et al., 2002; Klyachko and Stevens, 2003; Cherniak et al., 2004; Chklovskii and Koulakov, 2004; Cherniak, 2012) notwithstanding it small brain size.

Top-down and multisensory thalamocortical connections to S1

Subcortical projections can also provide important top-down recurrent inputs. Indeed, cortical connectivity also takes place through higher order thalamic nuclei such as the pulvinar through which cortico-thalamo-cortical loops are established (Sherman and Guillery, 2002; Sherman, 2005; Theyel et al., 2010; Sherman and Guillery, 2011; Saalman et al., 2012). The Po is such a higher order thalamic nucleus of the somatosensory system in the mouse (Hoogland et al., 1987; Diamond et al., 1992; Bourassa et al., 1995; Sherman and Guillery, 2006). The Po projections to the rostral and caudal barrel field were much stronger than to the non-barrel field somatosensory cortex. This could indicate that the barrel field might require more abundant indirect cortical information than the cortical representations of the rest of the body. The barrel field also receives more abundant projections from cortices dedicated to other sensory modalities and association cortices.

We also show here that the somatosensory cortex receives projections from both the Po and the visual higher-order thalamic lateral posterior nucleus which contrasts with the visual cortex that receives projections from the LP only (Charbonneau et al., 2012). The

visual LP in the mouse has been shown to provide contextual information on the speed of locomotion to the visual cortex (Roth et al., 2016). This information would be also conveyed to the somatosensory cortex and could be useful contextual information in whisking behavior.

Among the nuclei of the ventral thalamic group, VL sends a good number of projections to S1BF. It is well established that VL provides somatotopic motor information to the motor cortex (Strick, 1973; Schmahmann, 2003; Tlamsa and Brumberg, 2010), however, there is a small number of neurons in VL that projects to S1 (Donoghue et al., 1979; Spreafico et al., 1981). As we show here, this projection could target specifically S1BF. The functional role of VL projections to S1 is largely unknown, VL could be part of anatomical motor loops for eye blink conditioning (Sears et al., 1996), eye positioning (Werner-Reiss et al., 2003), and sensory motor task performance (Brosch et al., 2005).

Altogether, the mystacial caudal barrel field stands out from the rest of the primary somatosensory cortex by having more connections with cortical and subcortical visual structures such as V1 and LD. These projections could be the anatomical substrate of the influence of vision on the vibrissae tactile sensations and navigation in mice. The interaction of the vibrissae with vision could be important in the representation of the peripersonal space (Rizzolatti et al., 1981b; a), and which is specifically centered on the vibrissae in mice (Cardinali et al., 2009).

Conclusions

In conclusion, this study demonstrates the multitude and diversity of top-down and heteromodal cortical and subcortical projections to S1. This study demonstrates differences between the projections of the mystacial caudal barrel field, more rostral barrel field and somatosensory cortex outside the barrel field. S1 and the barrel field have afferent connections with somatosensory areas, non-somatosensory primary sensory areas, multisensory, motor, associative, and neuromodulatory areas but the caudal part of the barrel field displays more varied cortical and subcortical connections compared to the rest of S1. Indeed, when compared to the networks built from the Mouse Connectome Project data, a more caudal area such as the mystacial barrel field is a major component of the medial network which mediates transduction of information between the primary sensory areas and higher order association areas of the neocortex compared to the more rostral areas whose processes are more centered on somatosensory and motor information in the somatic sensorimotor network. The projections to S1 are mostly of a feedback nature, but exhibit a range of laminar indices. The primary auditory cortex projections were of feedback type whereas the visual projections towards the caudal part of the barrel field were more distinctly lateral supporting the different hierarchical positions of the primary sensory cortices. Along the previous studies on V1 and A1 in the mouse, this study demonstrates that associative and multisensory projections are present in all primary sensory cortices of the mouse and that these areas are not only dedicated to the processing of information of only one sensory modality.

Acknowledgements

We are grateful to Nadia Desnoyers for animal care and maintenance. This work was supported by discovery grants from the Natural Sciences and Engineering Research Council of Canada (NSERC) to DB and GB, and the Canadian Foundation for Innovation to DB. SBG was supported by the Réseau de la Recherche en Santé de la Vision (Fonds de la Recherche du Québec en Santé).

WITHDRAWN
see manuscript DOI for details

Table legends

TABLE 1: List of our cases that received CTb injections in the primary somatosensory cortex (S1) outside the barrel field, in the rostral (rS1BF) and caudal (cS1BF) barrel field and the cases used from the MCP corticocortical connectivity atlas that received CTb or Fluorogold (FG) injections in the primary somatosensory barrel field (SSp-bfd), lower limb (SSp-ll), and upper limb (SSp-ul) areas.

TABLE 2: Number and percentage (in parentheses) of retrogradely labeled neurons in sensory and non-sensory cortical areas in the ipsilateral hemisphere after injections of CTb into the primary somatosensory cortex (S1) of intact C57Bl/6 mice.

TABLE 3: Number and percentage (in parentheses) of retrogradely labeled neurons in sensory and non-sensory cortical areas in the contralateral hemisphere after injections of CTb into the primary somatosensory cortex (S1) of intact C57Bl/6 mice.

TABLE 4: Numbers of retrogradely labeled neurons in supragranular/infragranular layers and layer indices (below) in non-somatosensory sensory and non-sensory neocortical areas in the ipsilateral hemisphere after injections of CTb into S1, S1BF (rostral part) and S1BF (caudal part) of C57Bl/6 mice.

TABLE 5: Numbers of retrogradely labeled neurons in supragranular/infragranular layers and layer indices (below) in non-somatosensory sensory and non-sensory neocortical areas in the contralateral hemisphere after injections of CTb into S1, S1BF (rostral part) and S1BF (caudal part) of C57Bl/6 mice.

TABLE 6: Number and percentage (in parentheses) of retrogradely labeled neurons in sensory and non-sensory subcortical areas after injections of CTb into the primary somatosensory cortex (S1) of intact C57Bl/6 mice.

Figure legends

FIGURE 1: Tracer injection sites and distribution of retrogradely labeled neurons in the somatosensory thalamus. Photomicrographs of coronal sections from representative cases, showing CTb injection site in S1 (A), the rostral (B) and caudal (C) parts of the barrel field of S1 with retrogradely labeled neurons in VPL (D) and VPM (E/F) respectively. Scale: 1000 μm (A/B/C) and 200 μm (D/E/F).

FIGURE 2: CTb-labeled neurons in the cortex after an injection into the caudal part of the barrel field of S1. Scale: 250 μm .

FIGURE 3: Diagram of the afferent connections of the primary somatosensory cortex (S1) of the C57Bl/6 mouse. Each box represents a brain structure which is connected with S1 or the rostral or caudal parts of S1BF. The target of a projection is represented by an arrow. Checkmarks next to the boxes represent a brain structure which is connected with the barrel field or the lower or upper limb regions of S1 that was presented in the Mouse Connectome Project.

FIGURE 4: Percentage of retrogradely labeled neurons in cortical areas in the ipsilateral (A) and contralateral hemispheres (B).

FIGURE 5: Layer indices for neocortical areas in the ipsilateral (A) and contralateral hemispheres (B).

FIGURE 6: Layer indices matching between the ipsilateral hemisphere (X axis) and the contralateral hemisphere (Y axis). Each circle (S1), square (r S1BF) and diamond (c S1BF) represents the layer index of a cortical area for a single case in which retrogradely labeled neurons were plotted in both hemispheres.

FIGURE 7: Number of retrogradely labeled neurons (A/C/E) or layer indices (B/D/F) (Y axis) depending on their distance (X axis) from the injection site in S1 (A/B), the rostral (C/D) and caudal (E/F) parts of the barrel field of S1.

FIGURE 8: CTb-labeled neurons in the subcortex after an injection into the caudal part of the barrel field of S1. Scale: 250 μm .

FIGURE 9: Percentage of retrogradely labeled neurons in different subcortical areas.

FIGURE 10: Diagram showing the input ratios of different modalities into the primary somatosensory cortex of the C57Bl/6 mouse. Ratios were calculated from the relative numbers of retrogradely labeled neurons found in the respective structures.

CORTEX:

Somatosensory = S2 (S1 & S1BF only for the contralateral hemisphere).

Motor = M1, M2.

Multisensory = PtA, TeA, Cl, RSGc, RSD, Ect, PRh, PrL, IL, Orbital Cx, Insular Cx, DP, Cg.

Olfactory = Pir.

Auditory = Au.

Visual = V1, V2M, V2L.

Modulatory = No area.

SUBCORTEX:

Somatosensory = Po, VPL, VPM, APTD.

Motor = VL, VM, GP, ZI, CPu.

Multisensory = PT, Rt, Re, CPu, Rh.

Olfactory = No area.

Auditory = No area.

Visual = LD, LP.

Modulatory = AM, AHA, CM-PC, Hyp, Acb, AVVL, MD, LH, PVP, PM, mfb, VA.

WITHDRAWN
see manuscript DOI for details

Abbreviations

Acb	Accumbens nucleus
AHA	Anterior hypothalamic area
AI	Agranular insular cortex
AID	Agranular insular cortex, dorsal part
AIP	Agranular insular cortex, posterior part
AIV	Agranular insular cortex, ventral part
AM	Anteromedial thalamic nucleus
Amyg	Amygdala
AO	Anterior olfactory nucleus
AOM	Anterior olfactory nucleus, medial part
APTD	Anterior pretectal nucleus
Au	Auditory cortex
Au1	Primary auditory cortex
AuD	Secondary auditory cortex, dorsal part
AuV	Secondary auditory cortex, ventral part
AV	Anteroventral thalamic nucleus
AVVL	Anteroventral thalamic nucleus, ventrolateral part
Cg	Cingulate cortex
Cg1	Cingulate cortex, area I
Cl	Clastrum
CM-PC	Central medial thalamic nucleus
CPu	Caudate putamen (striatum)
Cu	Cuneate nucleus
DC	Dorsal peduncular cortex
Den	Dorsal endopiriform nucleus
DG	Dentate gyrus
DI	Dysgranular insular cortex
DP	Dorsal peduncular cortex
DTT	Dorsal tenia tecta
Ect	Ectorhinal cortex
Ent	Entorhinal cortex
EP	Entopeduncular nucleus
GI	Granular insular cortex
GP	Globus pallidus
Hyp	Hypothalamus
IC	Insular cortex
IL	Infralimbic cortex
LD	Laterodorsal thalamic nucleus
LH	Lateral hypothalamic area
LO	Lateral orbital cortex
LP	Lateral posterior thalamic nucleus
LSI	Lateral septal nucleus
M1	Primary motor cortex
M2	Secondary motor cortex
MCP	Mouse Connectome Project

MD	Mediodorsal thalamic nucleus
mfb	Medial forebrain bundle
mRt	Mesencephalic reticular formation
OC	Orbital cortex
Oth	Others
Pir	Piriform cortex
PM	Paramedian lobule
Pn	Pontine nuclei
Po	Posterior thalamic nuclear group
PRh	Perirhinal cortex
PrL	Prelimbic cortex
PT	Paratenial thalamic nucleus
PtA	Parietal association cortex
PVP	Paraventricular thalamic nucleus
Re	Reuniens thalamic nucleus
Rh	Rhomboid thalamic nucleus
R	Red nucleus
RSD	Retrosplenial dysgranular cortex
RSG	Retrosplenial granular cortex
Rt	Reticular nucleus (prethalamus)
S1	Primary somatosensory cortex
S2	Secondary somatosensory cortex
SC	Superior colliculus
SN	Substantia nigra
STh	Subthalamic nucleus
STLP	Bed nucleus of the stria terminalis
TeA	Temporal association cortex
V1	Primary visual cortex
V2L	Secondary visual cortex, lateral part
V2M	Secondary visual cortex, medial part
VA	Ventral anterior thalamic nucleus
VL	Ventrolateral thalamic nucleus
VM	Ventromedial thalamic nucleus
VO	Ventral orbital cortex
VP	Ventral pallidum
VPL	Ventral posterolateral thalamic nucleus
VPM	Ventral posteromedial thalamic nucleus
ZI	Zona incerta

Abbreviations from the Mouse Connectome Project

ACAd	Anterior cingulate area, dorsal part
Ald	Agranular insular area, dorsal part
Alp	Agranular insular area
Alv	Agranular insular area, ventral part
AONm	Anterior olfactory nucleus, medial part

AUDd	Dorsal auditory area
AUDp	Primary auditory area
AUDv	Ventral auditory area
CLA	Clastrum
DP	Dorsal peduncular area
ECT	Ectorhinal area
ENTI	Entorhinal area
EPd	Dorsal endopiriform nucleus
GU	Gustatory areas
ILA	Infralimbic area
Mop	Primary motor area
Mos	Secondary motor area
ORBI	Orbital area
ORBIvl	Orbital area, ventrolateral part
PTLp	Posterior parietal association areas
SSp	Primary somatosensory area
SSs	Secondary somatosensory area
Tea	Temporal association areas
TTd	Tenia tecta, dorsal part
VISal	Anterolateral visual area
VISam	Anteromedial visual area
VISl	Lateral visual area
VISp	Primary visual area
VISC	Visceral area

- Aggleton JP, Albasser MM, Aggleton DJ, Poirier GL, Pearce JM. 2010. Lesions of the rat perirhinal cortex spare the acquisition of a complex configural visual discrimination yet impair object recognition. *Behav Neurosci* 124(1):55-68.
- Bastos AM, Vezoli J, Bosman CA, Schoffelen JM, Oostenveld R, Dowdall JR, De Weerd P, Kennedy H, Fries P. 2015. Visual areas exert feedforward and feedback influences through distinct frequency channels. *Neuron* 85(2):390-401.
- Berezovskii VK, Nassi JJ, Born RT. 2011. Segregation of feedforward and feedback projections in mouse visual cortex. *J Comp Neurol* 519(18):3672-3683.
- Bollimunta A, Mo J, Schroeder CE, Ding M. 2011. Neuronal mechanisms and attentional modulation of corticothalamic alpha oscillations. *J Neurosci* 31(13):4935-4943.
- Bourassa J, Pinault D, Deschenes M. 1995. Corticothalamic projections from the cortical barrel field to the somatosensory thalamus in rats: a single-fibre study using biocytin as an anterograde tracer. *Eur J Neurosci* 7(1):19-30.
- Brosch M, Selezneva E, Scheich H. 2005. Nonauditory events of a behavioral procedure activate auditory cortex of highly trained monkeys. *J Neurosci* 25(29):6797-6806.
- Budinger E, Heil P, Hess A, Scheich H. 2006. Multisensory processing via early cortical stages: Connections of the primary auditory cortical field with other sensory systems. *Neuroscience* 143(4):1065-1083.
- Budinger E, Laszcz A, Lison H, Scheich H, Ohl FW. 2008. Non-sensory cortical and subcortical connections of the primary auditory cortex in Mongolian gerbils: bottom-up and top-down processing of neuronal information via field AI. *Brain Res* 1220:2-32.
- Budinger E, Scheich H. 2009. Anatomical connections suitable for the direct processing of neuronal information of different modalities via the rodent primary auditory cortex. *Hear Res* 258(1-2):16-27.
- Buffalo EA, Fries P, Landman R, Buschman TJ, Desimone R. 2011. Laminar differences in gamma and alpha coherence in the ventral stream. *Proc Natl Acad Sci U S A* 108(27):11262-11267.
- Bullier J. 2001. Integrated model of visual processing. *Brain Res Brain Res Rev* 36(2-3):96-107.
- Cardinali L, Brozzoli C, Farne A. 2009. Peripersonal space and body schema: two labels for the same concept? *Brain Topogr* 21(3-4):252-260.
- Caviness VS, Jr. 1975. Architectonic map of neocortex of the normal mouse. *J Comp Neurol* 164(2):247-263.
- Charbonneau V, Laramée ME, Boucher V, Bronchti G, Boire D. 2012. Cortical and subcortical projections to primary visual cortex in anophthalmic, enucleated and sighted mice. *Eur J Neurosci* 36(7):2949-2963.
- Cherniak C. 1994. Component placement optimization in the brain. *J Neurosci* 14(4):2418-2427.
- Cherniak C. 2012. Neural wiring optimization. *Prog Brain Res* 195:361-371.
- Cherniak C, Changizi M, Kang D. 1999. Large-scale optimization of neuron arbors. *Phys Rev E Stat Phys Plasmas Fluids Relat Interdiscip Topics* 59(5 Pt B):6001-6009.
- Cherniak C, Mokhtazada Z, Rodriguez-Esteban R, Changizi K. 2004. Global optimization of cerebral cortex layout. *Proc Natl Acad Sci U S A* 101(4):1081-1086.
- Chklovskii DB. 2000. Optimal sizes of dendritic and axonal arbors in a topographic projection. *J Neurophysiol* 83(4):2113-2119.
- Chklovskii DB, Koulakov AA. 2004. Maps in the brain: what can we learn from them? *Annu Rev Neurosci* 27:369-392.
- Chklovskii DB, Schikorski T, Stevens CF. 2002. Wiring optimization in cortical circuits. *Neuron* 34(3):341-347.

- Coogan TA, Burkhalter A. 1990. Conserved patterns of cortico-cortical connections define areal hierarchy in rat visual cortex. *Exp Brain Res* 80(1):49-53.
- Coogan TA, Burkhalter A. 1993. Hierarchical organization of areas in rat visual cortex. *J Neurosci* 13(9):3749-3772.
- Diamond ME, Armstrong-James M, Budway MJ, Ebner FF. 1992. Somatic sensory responses in the rostral sector of the posterior group (POm) and in the ventral posterior medial nucleus (VPM) of the rat thalamus: dependence on the barrel field cortex. *J Comp Neurol* 319(1):66-84.
- Dong H, Shao Z, Nerbonne JM, Burkhalter A. 2004. Differential depression of inhibitory synaptic responses in feedforward and feedback circuits between different areas of mouse visual cortex. *J Comp Neurol* 475(3):361-373.
- Donoghue JP, Kerman KL, Ebner FF. 1979. Evidence for two organizational plans within the somatic sensory-motor cortex of the rat. *J Comp Neurol* 183(3):647-663.
- Driver J, Noesselt T. 2008. Multisensory interplay reveals crossmodal influences on 'sensory-specific' brain regions, neural responses, and judgments. *Neuron* 57(1):11-23.
- Ercsey-Ravasz M, Markov NT, Lamy C, Van Essen DC, Knoblauch K, Toroczkai Z, Kennedy H. 2013. A predictive network model of cerebral cortical connectivity based on a distance rule. *Neuron* 80(1):184-197.
- Felleman DJ, Van Essen DC. 1991. Distributed hierarchical processing in the primate cerebral cortex. *Cereb Cortex* 1(1):1-47.
- Franklin BJ, Paxinos G. 2008. *The Mouse Brain in Stereotaxic Coordinates*. San Diego: Academic Press.
- Ghazanfar AA, Maier JX, Hoffman KL, Logothetis NK. 2005. Multisensory integration of dynamic faces and voices in rhesus monkey auditory cortex. *J Neurosci* 25(20):5004-5012.
- Gilbert CD, Li W. 2013. Top-down influences on visual processing. *Nat Rev Neurosci* 14(5):350-363.
- Gilbert CD, Sigman M. 2007. Brain states: top-down influences in sensory processing. *Neuron* 54(5):677-696.
- Godement P, Saillour P, Imbert M. 1979. Thalamic afferents to the visual cortex in congenitally anophthalmic mice. *Neurosci Lett* 13(3):271-278.
- Grossberg S. 1980. How does a brain build a cognitive code? *Psychol Rev* 87(1):1-51.
- Gutschalk A, Micheyl C, Oxenham AJ. 2008. Neural correlates of auditory perceptual awareness under informational masking. *PLoS Biol* 6(6):e138.
- Henschke JU, Noesselt T, Scheich H, Budinger E. 2015. Possible anatomical pathways for short-latency multisensory integration processes in primary sensory cortices. *Brain Struct Funct* 220(2):955-977.
- Hoogland PV, Welker E, Van der Loos H. 1987. Organization of the projections from barrel cortex to thalamus in mice studied with Phaseolus vulgaris-leucoagglutinin and HRP. *Exp Brain Res* 68(1):73-87.
- Hudetz AG, Vizuete JA, Imas OA. 2009. Desflurane selectively suppresses long-latency cortical neuronal response to flash in the rat. *Anesthesiology* 111(2):231-239.
- Ito M, Gilbert CD. 1999. Attention modulates contextual influences in the primary visual cortex of alert monkeys. *Neuron* 22(3):593-604.
- Jiang J, Summerfield C, Eger T. 2013. Attention sharpens the distinction between expected and unexpected percepts in the visual brain. *J Neurosci* 33(47):18438-18447.
- Klyachko VA, Stevens CF. 2003. Connectivity optimization and the positioning of cortical areas. *Proc Natl Acad Sci U S A* 100(13):7937-7941.

- Koulakov AA, Chklovskii DB. 2001. Orientation preference patterns in mammalian visual cortex: a wire length minimization approach. *Neuron* 29(2):519-527.
- Lee TS, Mumford D. 2003. Hierarchical Bayesian inference in the visual cortex. *J Opt Soc Am A Opt Image Sci Vis* 20(7):1434-1448.
- Llinas RR, Pare D. 1991. Of dreaming and wakefulness. *Neuroscience* 44(3):521-535.
- Makino H, Komiyama T. 2015. Learning enhances the relative impact of top-down processing in the visual cortex. *Nat Neurosci* 18(8):1116-1122.
- Markov NT, Vezoli J, Chameau P, Falchier A, Quilodran R, Huissoud C, Lamy C, Misery P, Giroud P, Ullman S, Barone P, Dehay C, Knoblauch K, Kennedy H. 2014. Anatomy of hierarchy: feedforward and feedback pathways in macaque visual cortex. *J Comp Neurol* 522(1):225-259.
- McManus JN, Li W, Gilbert CD. 2011. Adaptive shape processing in primary visual cortex. *Proc Natl Acad Sci U S A* 108(24):9739-9746.
- Meador KJ, Ray PG, Echaz J, Loring DW, Vachtsevanos GJ. 2002. Gamma coherence and conscious perception. *Neurology* 59(6):847-854.
- Meyer K. 2011. Primary sensory cortices, top-down projections and conscious experience. *Prog Neurobiol* 94(4):408-417.
- Michalareas G, Vezoli J, van Pelt S, Schoffelen JM, Kennedy H, Fries P. 2016. Alpha-Beta and Gamma Rhythms Subserve Feedback and Feedforward Influences among Human Visual Cortical Areas. *Neuron* 89(2):384-397.
- Mitchison G. 1991. Neuronal branching patterns and the economy of cortical wiring. *Proc Biol Sci* 245(1313):151-158.
- Moore C, Cavanagh P. 1998. Recovery of 3D volume from 2-tone images of novel objects. *Cognition* 67(1-2):45-71.
- Mumford D. 1992. On the computational architecture of the neocortex. II. The role of cortico-cortical loops. *Biol Cybern* 66(3):241-251.
- Naber PA, Witter MP, Lopes da Silva FH. 2000. Differential distribution of barrel or visual cortex. Evoked responses along the rostro-caudal axis of the peri- and postrhinal cortices. *Brain Res* 877(2):298-305.
- Rao RP, Ballard DH. 1999. Predictive coding in the visual cortex: a functional interpretation of some extra-classical receptive-field effects. *Nat Neurosci* 2(1):79-87.
- Rizzolatti G, Scandolara C, Matelli M, Gentilucci M. 1981a. Afferent properties of periarculate neurons in macaque monkeys. I. Somatosensory responses. *Behav Brain Res* 2(2):125-146.
- Rizzolatti G, Scandolara C, Matelli M, Gentilucci M. 1981b. Afferent properties of periarculate neurons in macaque monkeys. II. Visual responses. *Behav Brain Res* 2(2):147-163.
- Rockland KS, Pandya DN. 1979. Laminar origins and terminations of cortical connections of the occipital lobe in the rhesus monkey. *Brain Res* 179(1):3-20.
- Rodgers KM, Benison AM, Klein A, Barth DS. 2008. Auditory, somatosensory, and multisensory insular cortex in the rat. *Cereb Cortex* 18(12):2941-2951.
- Roelfsema PR, Lamme VA, Spekreijse H. 1998. Object-based attention in the primary visual cortex of the macaque monkey. *Nature* 395(6700):376-381.
- Roth MM, Dahmen JC, Muir DR, Imhof F, Martini FJ, Hofer SB. 2016. Thalamic nuclei convey diverse contextual information to layer 1 of visual cortex. *Nat Neurosci* 19(2):299-307.
- Saalman YB, Pinsk MA, Wang L, Li X, Kastner S. 2012. The pulvinar regulates information transmission between cortical areas based on attention demands. *Science* 337(6095):753-756.
- Schmahmann JD. 2003. Vascular syndromes of the thalamus. *Stroke* 34(9):2264-2278.

- Sears LL, Logue SF, Steinmetz JE. 1996. Involvement of the ventrolateral thalamic nucleus in rabbit classical eyeblink conditioning. *Behav Brain Res* 74(1-2):105-117.
- Sherman SM. 2005. Thalamic relays and cortical functioning. *Prog Brain Res* 149:107-126.
- Sherman SM, Guillery RW. 2002. The role of the thalamus in the flow of information to the cortex. *Philos Trans R Soc Lond B Biol Sci* 357(1428):1695-1708.
- Sherman SM, Guillery RW. 2006. Exploring the thalamus and its role in cortical function. Cambridge MA: MIT Press.
- Sherman SM, Guillery RW. 2011. Distinct functions for direct and transthalamic corticocortical connections. *J Neurophysiol* 106(3):1068-1077.
- Sieben K, Roder B, Hanganu-Opatz IL. 2013. Oscillatory entrainment of primary somatosensory cortex encodes visual control of tactile processing. *J Neurosci* 33(13):5736-5749.
- Spreafico R, Hayes NL, Rustioni A. 1981. Thalamic projections to the primary and secondary somatosensory cortices in cat: single and double retrograde tracer studies. *J Comp Neurol* 203(1):67-90.
- Strick PL. 1973. Light microscopic analysis of the cortical projection of the thalamic ventrolateral nucleus in the cat. *Brain Res* 55(1):1-24.
- Summerfield C, Egner T. 2009. Expectation (and attention) in visual cognition. *Trends Cogn Sci* 13(9):403-409.
- Super H, Spekreijse H, Lamme VA. 2001. Two distinct modes of sensory processing observed in monkey primary visual cortex (V1). *Nat Neurosci* 4(3):304-310.
- Teufel C, Nanay B. 2017. How to (and how not to) think about top-down influences on visual perception. *Conscious Cogn* 47:17-25.
- Theyel BB, Llano DA, Sherman SM. 2010. The corticothalamocortical circuit drives higher-order cortex in the mouse. *Nat Neurosci* 13(1):84-88.
- Tlamsa AP, Brumberg JC. 2010. Organization and morphology of thalamocortical neurons of mouse ventral lateral thalamus. *Somatosens Mot Res* 27(1):34-43.
- Tononi G, Koch C. 2008. The neural correlates of consciousness: an update. *Ann N Y Acad Sci* 1124:239-261.
- van Kerkoerle T, Self MW, Dagnino B, Gariel-Mathis MA, Poort J, van der Togt C, Roelfsema PR. 2014. Alpha and gamma oscillations characterize feedback and feedforward processing in monkey visual cortex. *Proc Natl Acad Sci U S A* 111(40):14332-14341.
- Werner-Reiss U, Kelly KA, Trause AS, Underhill AM, Groh JM. 2003. Eye position affects activity in primary auditory cortex of primates. *Curr Biol* 13(7):554-562.
- Winters BD, Saksida LM, Bussey TJ. 2008. Object recognition memory: neurobiological mechanisms of encoding, consolidation and retrieval. *Neurosci Biobehav Rev* 32(5):1055-1070.
- Xing D, Yeh CI, Burns S, Shapley RM. 2012. Laminar analysis of visually evoked activity in the primary visual cortex. *Proc Natl Acad Sci U S A* 109(34):13871-13876.
- Yamashita A, Valkova K, Gonchar Y, Burkhalter A. 2003. Rearrangement of synaptic connections with inhibitory neurons in developing mouse visual cortex. *J Comp Neurol* 464(4):426-437.
- Zakiewicz IM, Bjaalie JG, Leergaard TB. 2014. Brain-wide map of efferent projections from rat barrel cortex. *Front Neuroinform* 8:5.
- Zhang S, Xu M, Kamigaki T, Hoang Do JP, Chang WC, Jenvay S, Miyamichi K, Luo L, Dan Y. 2014. Selective attention. Long-range and local circuits for top-down modulation of visual cortex processing. *Science* 345(6197):660-665.

Zingg B, Hintiryan H, Gou L, Song MY, Bay M, Bienkowski MS, Foster NN, Yamashita S, Bowman I, Toga AW, Dong HW. 2014. Neural networks of the mouse neocortex. *Cell* 156(5):1096-1111.

WITHDRAWN
see manuscript DOI for details

TABLE 1: List of our cases that received CTB injections in the primary somatosensory cortex (S1) outside the barrel field, in the rostral (rS1BF) and caudal (cS1BF) barrel field and the cases used from the MCP corticocortical connectivity atlas that received CTB or Fluorogold (FG) injections in the primary somatosensory barrel field (SSp-bfd), lower limb (SSp-ll), and upper limb (SSp-ul) areas.

Our cases CTB injections			MCP cases				
Injection site	Case	Coordinates (mm) AP/ML/depth	Injection site	Case	Tracer	Coordinates (mm) AP/ML/depth	
S1	02-03a4	1.5/1.5/0.1-0.5	SSp-bfd	SW110420-01	CTB	4.0/-0.08/1.12	
	02-03a5	1.5/1.5/0.1-0.5		SW110322-04	NA	NA	
	02-03a3	1.5/1.5/0.1-0.5		SW110419-03	CTB	3.1/-0.88/0.9	
	02-03a6	1.5/1.5/0.1-0.5		SW110419-01	NA	NA	
	02-03a7	1.5/1.5/0.1-0.5		SW110322-01	NA	NA	
				SW110418-01	NA	NA	
				SW110420-03	NA	NA	
r S1BF	03-02b2	0.9/2.9/0.1-0.5	SSp-ll	SW110419-04	NA	NA	
	03-04a6	0.9/2.9/0.1-0.5		SSp-ul	SW110419-02	CTB	2.3/0.75/0.8
	03-04a7	0.9/2.9/0.1-0.5			SW110516-01	NA	NA
	03-04b4	0.9/2.9/0.1-0.5					
	03-04b5	0.9/2.9/0.1-0.5					
c S1BF	03-02b7	1.5/2.9/0.1-0.5					
	04-01b2	1.5/2.9/0.1-0.5					
	03-02b4	1.5/2.9/0.1-0.5					
	03-02b5	1.5/2.9/0.1-0.5					
	03-02b6	1.5/2.9/0.1-0.5					

TABLE 2: Number and percentage (in parentheses) of retrogradely labeled neurons in sensory and non-sensory cortical areas in the ipsilateral hemisphere after injections of CTb into the primary somatosensory cortex (S1) of intact C57Bl/6 mice.

Injection site	Case	Cortical area (ipsi)						
		M1	M2	S2	Au	V1	V2M	V2L
S1	02-03a4	638 (24.13)	148 (5.60)	720 (27.23)	584 (22.09)	0 (0)	0 (0)	0 (0)
	02-03a5	832 (22.75)	438 (11.97)	1736 (47.46)	140 (3.83)	0 (0)	0 (0)	0 (0)
	02-03a3	688 (22.21)	222 (7.17)	974 (31.44)	474 (15.30)	0 (0)	0 (0)	0 (0)
	02-03a6	368 (19.73)	147 (7.88)	614 (32.92)	181 (9.71)	0 (0)	0 (0)	0 (0)
	02-03a7	1176 (22.24)	549 (10.38)	2223 (42.05)	378 (7.15)	0 (0)	0 (0)	0 (0)
	Mean \pm SEM	740.40 \pm 147.91 (22.21 \pm 0.80)	300.80 \pm 91.39 (8.60 \pm 1.28)	1253.4 \pm 348.61 (36.22 \pm 4.14)	351.40 \pm 94.73 (11.61 \pm 3.60)	0 \pm 0 (0 \pm 0)	0 \pm 0 (0 \pm 0)	0 \pm 0 (0 \pm 0)
	r S1BF	03-02b2	170 (9.65)	832 (47.22)	296 (16.80)	0 (0)	0 (0)	0 (0)
	03-04a6	1376 (60.09)	122 (5.33)	492 (21.49)	6 (0.26)	0 (0)	0 (0)	0 (0)
	03-04a7	1650 (36.85)	1324 (29.57)	404 (9.02)	200 (4.47)	0 (0)	0 (0)	0 (0)
	03-04b4	1364 (30.41)	1416 (31.57)	736 (16.41)	50 (1.12)	0 (0)	0 (0)	0 (0)
	03-04b5	1060 (29.66)	1190 (33.30)	478 (13.37)	84 (2.35)	0 (0)	0 (0)	0 (0)
	Mean \pm SEM	1124.0 \pm 286.36 (33.33 \pm 9.05)	976.80 \pm 263.46 (29.40 \pm 7.57)	481.20 \pm 81.13 (15.42 \pm 2.30)	68.00 \pm 40.68 (1.64 \pm 0.91)	0 \pm 0 (0 \pm 0)	0 \pm 0 (0 \pm 0)	0 \pm 0 (0 \pm 0)
c S1BF	03-02b7	148 (7.18)	209 (10.14)	415 (20.14)	151 (7.33)	546 (26.49)	10 (0.46)	100 (4.85)
	04-01b2	726 (23.61)	573 (18.63)	582 (18.93)	365 (11.87)	76 (2.47)	8 (0.26)	37 (1.20)
	03-02b4	800 (13.69)	1510 (25.85)	600 (10.27)	409 (7.00)	400 (6.85)	69 (1.18)	230 (3.94)
	03-02b5	929 (14.88)	1197 (19.16)	1181 (18.91)	1063 (17.02)	154 (2.47)	93 (1.49)	115 (1.84)
	03-02b6	450 (16.43)	323 (11.79)	1117 (40.78)	121 (4.42)	33 (1.21)	3 (0.11)	20 (0.73)
	Mean \pm SEM	610.60 \pm 156.20 (15.16 \pm 2.95)	762.40 \pm 283.17 (17.12 \pm 3.16)	779.00 \pm 173.06 (21.80 \pm 5.67)	421.80 \pm 190.12 (9.53 \pm 2.49)	241.80 \pm 110.78 (7.90 \pm 5.31)	36.60 \pm 20.74 (0.71 \pm 0.30)	100.40 \pm 41.45 (2.51 \pm 0.90)

Injection site	Case	Cortical area (ipsi)						
		PtA	TeA	RSGc	RSD	Ect	PRh	Pir
S1	02-03a4	218 (8.25)	108 (4.09)	0 (0)	0 (0)	194 (7.34)	0 (0)	0 (0)
	02-03a5	236 (6.45)	12 (0.33)	6 (0.16)	32 (0.88)	104 (2.84)	22 (0.60)	6 (0.16)
	02-03a3	224 (7.23)	84 (2.71)	8 (0.26)	36 (1.16)	172 (5.55)	114 (3.68)	19 (0.61)
	02-03a6	114 (6.11)	30 (1.61)	8 (0.43)	26 (1.39)	75 (4.02)	42 (2.25)	7 (0.38)
	02-03a7	348 (6.58)	57 (1.08)	9 (0.17)	37 (0.70)	192 (3.63)	67 (1.27)	16 (0.30)
	Mean ± SEM	228.00 ± 41.52 (6.92 ± 0.42)	58.20 ± 19.49 (1.96 ± 0.74)	6.20 ± 1.82 (0.20 ± 0.08)	26.20 ± 7.64 (0.83 ± 0.27)	147.40 ± 27.26 (4.68 ± 0.89)	49.00 ± 21.98 (1.56 ± 0.73)	9.60 ± 3.88 (0.29 ± 0.12)
r S1BF	03-02b2	0 (0)	0 (0)	0 (0)	0 (0)	36 (2.04)	44 (2.50)	26 (1.48)
	03-04a6	0 (0)	2 (0.09)	0 (0)	2 (0.09)	80 (3.49)	78 (4.41)	4 (0.18)
	03-04a7	92 (2.05)	18 (0.40)	10 (0.22)	40 (0.89)	418 (9.34)	186 (4.15)	32 (0.72)
	03-04b4	0 (0)	10 (0.22)	12 (0.27)	36 (0.80)	230 (5.13)	72 (1.61)	10 (0.22)
	03-04b5	30 (0.84)	10 (0.28)	8 (0.22)	26 (0.73)	228 (6.38)	100 (2.80)	22 (0.62)
	Mean ± SEM	24.40 ± 19.98 (0.58 ± 0.45)	8.00 ± 3.61 (0.20 ± 0.08)	6.00 ± 2.83 (0.14 ± 0.07)	20.80 ± 9.40 (0.50 ± 0.21)	198.40 ± 75.20 (5.28 ± 1.40)	96.00 ± 27.07 (2.89 ± 0.48)	18.80 ± 5.77 (0.64 ± 0.26)
c S1BF	03-02b7	13 (0.63)	42 (2.04)	8 (0.39)	14 (0.68)	215 (10.43)	42 (2.04)	77 (3.74)
	04-01b2	185 (6.02)	88 (2.86)	4 (0.13)	24 (0.78)	245 (7.97)	36 (1.17)	65 (2.11)
	03-02b4	168 (2.88)	145 (2.48)	37 (0.63)	146 (2.50)	274 (4.69)	48 (0.82)	111 (1.90)
	03-02b5	352 (5.64)	234 (3.75)	70 (1.12)	163 (2.61)	231 (3.70)	67 (1.07)	189 (3.03)
	03-02b6	166 (6.06)	17 (0.62)	4 (0.15)	23 (0.84)	235 (8.58)	92 (3.36)	56 (2.04)
	Mean ± SEM	176.80 ± 60.10 (4.24 ± 1.21)	105.20 ± 43.48 (2.35 ± 0.58)	24.60 ± 14.45 (0.48 ± 0.21)	74.00 ± 36.92 (1.48 ± 0.49)	240.00 ± 10.93 (7.07 ± 1.40)	57.00 ± 11.38 (1.69 ± 0.52)	99.60 ± 27.08 (2.56 ± 0.40)

Injection site	Case	Cortical area (ipsi)						
		Amyg	PrL	IL	Orbital Cx	Insular Cx	CI	DP
S1	02-03a4	2 (0.08)	0 (0)	0 (0)	0 (0)	0 (0)	8 (0.30)	0 (0)
	02-03a5	4 (0.11)	0 (0)	16 (0.44)	6 (0.16)	4 (0.11)	46 (1.26)	0 (0)
	02-03a3	6 (0.19)	0 (0)	8 (0.26)	3 (0.10)	9 (0.29)	18 (0.58)	0 (0)
	02-03a6	14 (0.75)	0 (0)	4 (0.22)	192 (10.30)	18 (0.97)	14 (0.75)	0 (0)
	02-03a7	12 (0.23)	0 (0)	12 (0.23)	87 (1.65)	32 (0.61)	57 (1.08)	0 (0)
	Mean ± SEM	7.60 ± 2.59 (0.27 ± 0.14)	0 ± 0 (0 ± 0)	8.00 ± 3.16 (0.23 ± 0.08)	57.60 ± 41.75 (2.44 ± 2.22)	12.60 ± 6.38 (0.39 ± 0.20)	28.60 ± 10.78 (0.79 ± 0.19)	0 ± 0 (0 ± 0)
r S1BF	03-02b2	22 (1.25)	0 (0)	0 (0)	112 (6.36)	124 (7.04)	100 (5.68)	0 (0)
	03-04a6	4 (0.18)	0 (0)	0 (0)	32 (1.40)	34 (1.49)	58 (2.53)	0 (0)
	03-04a7	8 (0.18)	0 (0)	0 (0)	0 (0)	14 (0.31)	30 (0.67)	16 (0.36)
	03-04b4	26 (0.58)	0 (0)	0 (0)	380 (8.47)	34 (0.76)	110 (2.45)	0 (0)
	03-04b5	18 (0.50)	0 (0)	0 (0)	164 (4.59)	58 (1.62)	80 (2.24)	3 (0.17)
	Mean ± SEM	15.60 ± 4.66 (0.54 ± 0.22)	0 ± 0 (0 ± 0)	0 ± 0 (0 ± 0)	137.60 ± 75.08 (4.16 ± 1.74)	52.80 ± 21.37 (2.24 ± 1.37)	75.60 ± 16.18 (2.71 ± 0.91)	4.40 ± 3.49 (0.11 ± 0.08)
c S1BF	03-02b7	2 (0.10)	0 (0)	0 (0)	39 (1.89)	9 (0.44)	21 (1.02)	0 (0)
	04-01b2	1 (0.03)	0 (0)	0 (0)	26 (0.85)	1 (0.03)	33 (1.07)	0 (0)
	03-02b4	42 (0.72)	1 (0.02)	6 (0.10)	623 (10.66)	39 (0.67)	143 (2.45)	8 (0.14)
	03-02b5	5 (0.08)	5 (0.08)	11 (0.18)	72 (1.15)	0 (0)	84 (1.35)	1 (0.02)
	03-02b6	1 (0.04)	0 (0)	0 (0)	20 (0.73)	4 (0.15)	48 (1.75)	6 (0.22)
	Mean ± SEM	10.20 ± 8.93 (0.19 ± 0.15)	1.20 ± 1.08 (0.02 ± 0.02)	3.40 ± 2.49 (0.06 ± 0.04)	156.00 ± 130.92 (3.06 ± 2.14)	10.60 ± 8.13 (0.26 ± 0.14)	65.80 ± 24.61 (1.53 ± 0.30)	3.00 ± 1.87 (0.07 ± 0.05)

Injection site	Case	Cortical area (ipsi)
		Cg
S1	02-03a4	0 (0)
	02-03a5	18 (0.49)
	02-03a3	27 (0.87)
	02-03a6	5 (0.27)
	02-03a7	17 (0.32)
	Mean ± SEM	13.40 ± 5.42 (0.39 ± 0.16)
r S1BF	03-02b2	0 (0)
	03-04a6	0 (0)
	03-04a7	36 (0.80)
	03-04b4	0 (0)
	03-04b5	6 (0.34)
	Mean ± SEM	9.60 ± 7.82 (0.23 ± 0.18)
c S1BF	03-02b7	0 (0)
	04-01b2	0 (0)
	03-02b4	33 (0.57)
	03-02b5	31 (0.50)
	03-02b6	0 (0)
	Mean ± SEM	12.80 ± 8.77 (0.21 ± 0.15)

WITHDRAWN
see manuscript DOI for details

TABLE 3: Number and percentage (in parentheses) of retrogradely labeled neurons in sensory and non-sensory cortical areas in the contralateral hemisphere after injections of CTb into the primary somatosensory cortex (S1) of intact C57Bl/6 mice.

Injection site	Case	Cortical area (con)							
		S1	S1BF	M1	M2	S2	Au	V1	
S1	02-03a4	244 (61.93)	6 (1.52)	70 (17.77)	60 (15.23)	8 (2.03)	4 (1.02)	0 (0)	
	02-03a5	364 (46.13)	7 (0.89)	206 (26.11)	132 (16.73)	10 (1.27)	0 (0)	0 (0)	
	02-03a3	287 (36.89)	7 (0.90)	104 (13.37)	78 (10.03)	10 (1.29)	4 (0.51)	0 (0)	
	02-03a6	165 (42.20)	4 (1.02)	69 (17.65)	48 (12.28)	5 (1.28)	2 (0.51)	0 (0)	
	02-03a7	521 (44.08)	11 (0.93)	258 (21.83)	171 (14.47)	15 (1.27)	6 (0.51)	0 (0)	
	Mean \pm SEM	316.20 \pm 67.62 (46.25 \pm 4.71)	7.00 \pm 1.28 (1.05 \pm 0.13)	141.40 \pm 42.94 (19.34 \pm 2.41)	97.80 \pm 26.02 (13.75 \pm 1.31)	9.60 \pm 1.82 (1.43 \pm 0.17)	3.20 \pm 1.14 (0.51 \pm 0.18)	0 \pm 0 (0 \pm 0)	
	r S1BF	03-02b2	42 (6.09)	272 (39.42)	8 (1.16)	0 (0)	162 (23.48)	0 (0)	0 (0)
	03-04a6	173 (13.58)	637 (50.00)	132 (10.36)	8 (0.63)	110 (8.63)	0 (0)	0 (0)	
	03-04a7	90 (7.65)	53 (4.50)	162 (13.76)	100 (8.50)	20 (1.70)	0 (0)	0 (0)	
	03-04b4	385 (13.57)	1350 (47.59)	324 (11.42)	114 (4.02)	304 (10.72)	0 (0)	0 (0)	
	03-04b5	177 (11.12)	579 (36.37)	164 (10.30)	72 (4.52)	162 (10.18)	0 (0)	0 (0)	
	Mean \pm SEM	173.40 \pm 65.67 (10.40 \pm 1.71)	578.20 \pm 246.06 (35.58 \pm 9.13)	158.00 \pm 56.34 (9.40 \pm 2.41)	58.80 \pm 26.17 (3.53 \pm 1.71)	151.60 \pm 51.53 (10.94 \pm 3.94)	0 \pm 0 (0 \pm 0)	0 \pm 0 (0 \pm 0)	
c S1BF	03-02b7	36 (9.65)	62 (16.62)	19 (5.09)	183 (49.06)	17 (4.56)	0 (0)	0 (0)	
	04-01b2	44 (0)	59 (0)	43 (20.38)	14 (6.64)	16 (7.58)	4 (1.90)	0 (0)	
	03-02b4	244 (0)	427 (0)	129 (16.69)	124 (16.04)	117 (15.14)	25 (3.23)	0 (0)	
	03-02b5	64 (0)	103 (0)	42 (11.35)	36 (9.73)	28 (7.57)	24 (6.49)	0 (0)	
	03-02b6	21 (0)	22 (0)	24 (14.46)	13 (7.83)	6 (3.62)	0 (0)	0 (0)	
	Mean \pm SEM	81.80 \pm 46.00 (12.51 \pm 1.50)	134.6 \pm 82.98 (18.94 \pm 3.44)	51.40 \pm 22.33 (9.41 \pm 1.66)	74.00 \pm 38.04 (15.01 \pm 9.55)	36.80 \pm 22.75 (5.17 \pm 0.94)	10.60 \pm 6.40 (1.50 \pm 0.92)	0 \pm 0 (0 \pm 0)	

Injection site	Case	Cortical area (con)						
		V2M	V2L	PtA	TeA	RSGc	RSD	Ect
S1	02-03a4	0 (0)	0 (0)	0 (0)	0 (0)	0 (0)	0 (0)	2 (0.51)
	02-03a5	0 (0)	0 (0)	0 (0)	0 (0)	0 (0)	16 (2.03)	14 (1.77)
	02-03a3	0 (0)	0 (0)	0 (0)	0 (0)	0 (0)	8 (1.03)	6 (0.77)
	02-03a6	0 (0)	0 (0)	0 (0)	0 (0)	0 (0)	4 (1.02)	4 (1.02)
	02-03a7	0 (0)	0 (0)	0 (0)	0 (0)	0 (0)	12 (1.02)	18 (1.52)
	Mean ± SEM	0 ± 0 (0 ± 0)	0 ± 0 (0 ± 0)	0 ± 0 (0 ± 0)	0 ± 0 (0 ± 0)	0 ± 0 (0 ± 0)	0 ± 0 (0 ± 0)	8.00 ± 3.16 (1.02 ± 0.36)
r S1BF	03-02b2	0 (0)	0 (0)	0 (0)	0 (0)	0 (0)	0 (0)	26 (3.77)
	03-04a6	0 (0)	0 (0)	0 (0)	4 (0.31)	0 (0)	0 (0)	80 (6.28)
	03-04a7	0 (0)	0 (0)	0 (0)	0 (0)	0 (0)	0 (0)	116 (9.86)
	03-04b4	0 (0)	0 (0)	0 (0)	6 (0.21)	0 (0)	0 (0)	86 (3.03)
	03-04b5	0 (0)	0 (0)	0 (0)	2 (0.13)	0 (0)	0 (0)	76 (4.77)
	Mean ± SEM	0 ± 0 (0 ± 0)	0 ± 0 (0 ± 0)	0 ± 0 (0 ± 0)	2.40 ± 1.30 (0.13 ± 0.07)	0 ± 0 (0 ± 0)	0 ± 0 (0 ± 0)	0 ± 0 (0 ± 0)
c S1BF	03-02b7	0 (0)	0 (0)	1 (0.27)	1 (0.27)	0 (0)	1 (0.27)	44 (11.80)
	04-01b2	0 (0)	0 (0)	0 (0)	3 (1.42)	2 (0.95)	6 (2.84)	43 (20.38)
	03-02b4	0 (0)	0 (0)	15 (1.94)	4 (0.52)	2 (0.26)	14 (1.81)	149 (19.28)
	03-02b5	0 (0)	0 (0)	9 (2.43)	13 (3.51)	0 (0)	1 (0.27)	55 (14.87)
	03-02b6	0 (0)	0 (0)	0 (0)	0 (0)	0 (0)	1 (0.60)	8 (4.82)
	Mean ± SEM	0 ± 0 (0 ± 0)	0 ± 0 (0 ± 0)	5.00 ± 3.37 (0.60 ± 0.37)	4.20 ± 2.58 (0.78 ± 0.49)	0.80 ± 0.55 (0.16 ± 0.14)	4.60 ± 2.84 (0.76 ± 0.36)	59.80 ± 26.45 (9.98 ± 1.86)

Injection site	Case	Cortical area (con)						
		PRh	Pir	Amyg	PrL	IL	Orbital Cx	Insular Cx
S1	02-03a4	0 (0)	0 (0)	0 (0)	0 (0)	0 (0)	0 (0)	0 (0)
	02-03a5	32 (4.06)	0 (0)	0 (0)	0 (0)	0 (0)	8 (1.01)	0 (0)
	02-03a3	270 (34.70)	0 (0)	0 (0)	0 (0)	0 (0)	4 (0.51)	0 (0)
	02-03a6	67 (17.14)	0 (0)	0 (0)	0 (0)	0 (0)	23 (5.88)	0 (0)
	02-03a7	157 (13.28)	0 (0)	0 (0)	0 (0)	0 (0)	13 (1.10)	0 (0)
	Mean ± SEM	105.20 ± 54.62 (13.84 ± 6.77)	0 ± 0 (0 ± 0)	0 ± 0 (0 ± 0)	0 ± 0 (0 ± 0)	0 ± 0 (0 ± 0)	9.60 ± 4.45 (1.70 ± 1.19)	0 ± 0 (0 ± 0)
r S1BF	03-02b2	174 (25.22)	0 (0)	4 (0.58)	0 (0)	0 (0)	0 (0)	0 (0)
	03-04a6	90 (7.06)	2 (0.16)	2 (0.16)	0 (0)	0 (0)	0 (0)	34 (2.67)
	03-04a7	508 (43.16)	12 (1.02)	8 (0.68)	0 (0)	0 (0)	0 (0)	108 (9.18)
	03-04b4	118 (4.16)	20 (0.71)	10 (0.35)	2 (0.07)	0 (0)	42 (1.48)	70 (2.47)
	03-04b5	266 (16.71)	10 (0.63)	8 (0.50)	0 (0)	0 (0)	14 (0.88)	60 (3.77)
	Mean ± SEM	231.20 ± 84.36 (19.26 ± 7.87)	8.80 ± 4.04 (0.50 ± 0.21)	6.40 ± 1.64 (0.45 ± 0.10)	0.40 ± 0.45 (0.01 ± 0.02)	0 ± 0 (0 ± 0)	11.20 ± 9.13 (0.47 ± 0.34)	54.40 ± 20.19 (3.62 ± 1.70)
c S1BF	03-02b7	4 (1.07)	2 (0.54)	1 (0.27)	1 (0.27)	1 (0.27)	0 (0)	0 (0)
	04-01b2	17 (8.06)	4 (1.90)	0 (0)	0 (0)	0 (0)	15 (7.11)	12 (5.69)
	03-02b4	101 (13.07)	2 (0.26)	0 (0)	0 (0)	0 (0)	55 (7.12)	12 (1.55)
	03-02b5	106 (28.65)	36 (9.73)	0 (0)	0 (0)	0 (0)	18 (4.87)	0 (0)
	03-02b6	34 (20.48)	7 (4.22)	0 (0)	0 (0)	0 (0)	10 (6.02)	62 (4.82)
	Mean ± SEM	52.40 ± 23.94 (9.90 ± 3.90)	10.20 ± 7.28 (2.40 ± 1.35)	0.20 ± 0.22 (0.05 ± 0.06)	0.20 ± 0.22 (0.05 ± 0.06)	0.20 ± 0.22 (0.05 ± 0.06)	19.60 ± 10.47 (3.35 ± 0.99)	17.20 ± 12.88 (6.86 ± 6.42)

Injection site	Case	Cortical area (con)		
		Cl	DP	Cg
S1	02-03a4	0 (0)	0 (0)	0 (0)
	02-03a5	0 (0)	0 (0)	0 (0)
	02-03a3	0 (0)	0 (0)	0 (0)
	02-03a6	0 (0)	0 (0)	0 (0)
	02-03a7	0 (0)	0 (0)	0 (0)
	Mean ± SEM	0 ± 0 (0 ± 0)	0 ± 0 (0 ± 0)	0 ± 0 (0 ± 0)
r S1BF	03-02b2	2 (0.29)	0 (0)	0 (0)
	03-04a6	0 (0)	0 (0)	2 (0.16)
	03-04a7	0 (0)	0 (0)	0 (0)
	03-04b4	6 (0.21)	0 (0)	0 (0)
	03-04b5	2 (0.13)	0 (0)	0 (0)
	Mean ± SEM	2.00 ± 1.23 (0.13 ± 0.06)	0 ± 0 (0 ± 0)	0.40 ± 0.45 (0.03 ± 0.04)
c S1BF	03-02b7	0 (0)	0 (0)	0 (0)
	04-01b2	32 (15.17)	0 (0)	0 (0)
	03-02b4	24 (3.11)	0 (0)	0 (0)
	03-02b5	2 (0.54)	0 (0)	0 (0)
	03-02b6	1 (20.48)	0 (0)	0 (0)
	Mean ± SEM	11.80 ± 7.54 (2.54 ± 2.16)	0 ± 0 (0 ± 0)	0 ± 0 (0 ± 0)

TABLE 4: Numbers of retrogradely labeled neurons in supragranular/infragranular layers and layer indices (below) in non-somatosensory sensory and non-sensory neocortical areas in the ipsilateral hemisphere after injections of CTb into S1, S1BF (rostral part) and S1BF (caudal part) of C57Bl/6 mice.

Injection site	Case	Cortical area (ipsi)			
		M1	M2	S2	Au
S1	02-03a4	242 / 396	36 / 112	98 / 456	74 / 470
		-0.24	-0.51	-0.65	-0.73
	02-03a5	291 / 541	154 / 284	506 / 858	6 / 98
		-0.30	-0.30	-0.26	-0.89
	02-03a3	255 / 433	66 / 156	200 / 558	58 / 378
		-0.26	-0.41	-0.47	-0.73
	02-03a6	133 / 235	48 / 99	151 / 329	20 / 143
	-0.28	-0.35	-0.37	-0.76	
	02-03a7	419 / 757	187 / 362	606 / 1140	36 / 291
		-0.29	-0.32	-0.31	-0.78
	Mean ± SEM	268 ± 52/472 ± 97 -0.28 ± 0.01	98 ± 34/203 ± 58 -0.35 ± 0.04	312 ± 114/668 ± 167 -0.37 ± 0.08	39 ± 14/276 ± 82 -0.75 ± 0.03
r S1BF	03-02b2	44 / 126	280 / 552	30 / 138	
		-0.48	-0.33	-0.64	
	03-04a6	416 / 960	24 / 98	88 / 342	0 / 6
		-0.40	-0.61	-0.59	-1.00
	03-04a7	563 / 1087	386 / 938	20 / 324	8 / 144
		-0.32	-0.42	-0.88	-0.90
	03-04b4	263 / 1101	194 / 1222	86 / 474	8 / 30
	-0.61	-0.73	-0.69	-0.58	
	03-04b5	289 / 771	286 / 904	46 / 312	6 / 58
		-0.46	-0.52	-0.74	-0.81
	Mean ± SEM	315 ± 96/809 ± 205 -0.44 ± 0.06	234 ± 24/743 ± 224 -0.52 ± 0.09	54 ± 16/318 ± 60 -0.71 ± 0.06	6 ± 2/60 ± 29 -0.83 ± 0.09
c S1BF	03-02b7	81 / 67	103 / 106	38 / 351	1 / 127
		0.10	-0.01	-0.80	-0.98
	04-01b2	332 / 394	340 / 233	122 / 413	19 / 247
		-0.09	0.19	-0.54	-0.86
	03-02b4	127 / 673	259 / 1251	124 / 436	14 / 295
		-0.68	-0.66	-0.56	-0.91
	03-02b5	405 / 524	551 / 646	373 / 733	119 / 675
	-0.13	-0.08	-0.33	-0.70	
	03-02b6	167 / 283	133 / 178	169 / 888	3 / 94
		-0.26	-0.18	-0.68	-0.94
	Mean ± SEM	222 ± 70/388 ± 130 -0.27 ± 0.15	277 ± 90/485 ± 239 -0.27 ± 0.16	165 ± 63/564 ± 134 -0.55 ± 0.09	31 ± 25/288 ± 119 -0.80 ± 0.06

Injection site	Case	Cortical area (ipsi)			
		V1	V2M	V2L	PtA
S1	02-03a4				58 / 116 -0.33
	02-03a5				42 / 124 -0.49
	02-03a3				54 / 118 -0.37
	02-03a6				25 / 60 -0.41
	02-03a7				69 / 183 -0.45
	Mean ± SEM				50 ± 8/120 ± 23 -0.41 ± 0.03
	r S1BF	03-02b2			
	03-04a6				
	03-04a7				34 / 40 -0.08
	03-04b4				
	03-04b5				12 / 12 0.00
	Mean ± SEM				23 ± 7/26 ± 9 -0.06 ± 0.02
c S1BF	03-02b7	216 / 236 -0.04	3 / 3 0.00	14 / 42 -0.50	4 / 7 -0.27
	04-01b2	34 / 39 -0.07	6 / 1 0.71	2 / 26 -0.86	51 / 72 -0.17
	03-02b4	157 / 203 -0.13	11 / 43 -0.59	30 / 150 -0.67	29 / 114 -0.59
	03-02b5	79 / 60 0.14	34 / 28 0.10	51 / 45 0.06	39 / 237 -0.72
	03-02b6	16 / 12 0.14	1 / 2 -0.33	3 / 12 -0.6	69 / 75 -0.04
	Mean ± SEM	100 ± 42/110 ± 51 -0.05 ± 0.06	11 ± 7/15 ± 10 -0.17 ± 0.25	20 ± 10/55 ± 27 -0.47 ± 0.17	38 ± 12/101 ± 44 -0.45 ± 0.14

Injection site	Case	Cortical area (ipsi)
		TeA
S1	02-03a4	2 / 98 -0.96
	02-03a5	0 / 12 -1.00
	02-03a3	2 / 78 -0.95
	02-03a6	1 / 28 -0.93
	02-03a7	3 / 54 -0.90
	Mean ± SEM	2 ± 1/54 ± 18 -0.94 ± 0.02
	r S1BF	03-02b2
	03-04a6	
	03-04a7	2 / 16 -0.78
	03-04b4	0 / 6 -1.00
	03-04b5	0 / 6 -1.00
	Mean ± SEM	1 ± 0/7 ± 4 -0.87 ± 0.24
c S1BF	03-02b7	0 / 33 -1.00
	04-01b2	0 / 77 -1.00
	03-02b4	12 / 103 -0.79
	03-02b5	7 / 192 -0.93
	03-02b6	0 / 14 -1.00
	Mean ± SEM	4 ± 3/84 ± 36 -0.91 ± 0.05

TABLE 5: Numbers of retrogradely labeled neurons in supragranular/infragranular layers and layer indices (below) in non-somatosensory sensory and non-sensory neocortical areas in the contralateral hemisphere after injections of CTb into S1, S1BF (rostral part) and S1BF (caudal part) of C57Bl/6 mice.

Injection site	Case	Cortical area (con)			
		S1	S1BF	M1	M2
S1	02-03a4	141 / 58	1 / 4	52 / 18	23 / 37
		0.42	-0.60	0.49	-0.23
	02-03a5	199 / 99	2 / 3	113 / 93	36 / 96
		0.34	-0.20	0.10	-0.46
	02-03a3	167 / 72	2 / 3	67 / 37	26 / 52
		0.40	-0.20	0.29	-0.33
	02-03a6	93 / 43	1 / 1	41 / 28	15 / 33
	0.37	0.00	0.19	-0.38	
	02-03a7	289 / 140	4 / 6	147 / 111	50 / 121
		0.35	-0.20	0.14	-0.42
	Mean ± SEM	178 ± 37/83 ± 19	2 ± 1/3 ± 1	84 ± 22/57 ± 21	30 ± 7/68 ± 21
		0.37 ± 0.02	-0.26 ± 0.11	0.19 ± 0.08	-0.39 ± 0.04
r S1BF	03-02b2	14 / 24	56 / 200	0 / 8	
		-0.26	-0.56	-1.00	
	03-04a6	20 / 131	69 / 547	14 / 118	2 / 6
		-0.74	-0.78	-0.79	-0.50
	03-04a7	12 / 60	12 / 36	28 / 134	13 / 87
		-0.67	-0.50	-0.65	-0.74
	03-04b4	57 / 299	187 / 1099	23 / 301	6 / 108
	-0.68	-0.71	-0.86	-0.90	
	03-04b5	33 / 128	102 / 445	18 / 146	6 / 66
		-0.59	-0.63	-0.78	-0.83
	Mean ± SEM	27 ± 9/128 ± 54	85 ± 33/465 ± 201	17 ± 5/141 ± 54	7 ± 3/67 ± 26
		-0.65 ± 0.09	-0.69 ± 0.06	-0.79 ± 0.06	-0.82 ± 0.09
c S1BF	03-02b7	20 / 13	15 / 42	5 / 14	101 / 82
		0.21	-0.47	-0.48	0.10
	04-01b2	18 / 26	14 / 38	3 / 40	12 / 2
		-0.18	-0.46	-0.86	0.71
	03-02b4	121 / 110	108 / 288	5 / 124	16 / 108
		0.05	-0.46	-0.92	-0.74
	03-02b5	33 / 23	29 / 63	12 / 30	17 / 19
	0.18	-0.37	-0.43	-0.06	
	03-02b6	10 / 9	5 / 15	9 / 15	5 / 8
		0.05	-0.50	-0.25	-0.23
	Mean ± SEM	40 ± 23/36 ± 21	171 ± 21/446 ± 56	7 ± 2/45 ± 23	30 ± 20/44 ± 25
		0.06 ± 0.08	-0.45 ± 0.03	-0.74 ± 0.15	-0.18 ± 0.27

Injection site	Case	Cortical area (con)			
		S2	Au	PtA	TeA
S1	02-03a4	2 / 6 -0.50	0 / 4 -1.00		
	02-03a5	4 / 6 -0.20			
	02-03a3	4 / 6 -0.20	0 / 4 -1.00		
	02-03a6	2 / 3 -0.20	0 / 2 -1.00		
	02-03a7	6 / 9 -0.20	0 / 6 -1.00		
	Mean ± SEM	4 ± 1/6 ± 1 -0.25 ± 0.07	0 ± 0/4 ± 1 -1.00 ± 0.00		
	r S1BF	03-02b2	12 / 146 -0.85		
	03-04a6	0 / 108 -1.00			
	03-04a7	0 / 20 -1.00			
	03-04b4	0 / 284 -1.00			0 / 2 -1.00
	03-04b5	4 / 150 -0.95			
	Mean ± SEM	3 ± 3/142 ± 56 -0.96 ± 0.03			0 ± 0/2 ± 0 -1.00 ± 0.00
c S1BF	03-02b7	1 / 16 -0.88		1 / 0 1.00	1 / 0 1.00
	04-01b2	0 / 12 -1.00	0 / 4 -1.00		1 / 2 -0.33
	03-02b4	11 / 95 -0.79	1 / 24 -0.92	5 / 8 -0.23	0 / 3 -1.00
	03-02b5	8 / 12 -0.20	1 / 23 -0.92	0 / 6 -1.00	0 / 10 -1.00
	03-02b6	0 / 5 -1.00			
	Mean ± SEM	4 ± 3/28 ± 19 -0.75 ± 0.17	1 ± 0/17 ± 7 -0.93 ± 0.02	2 ± 1/5 ± 3 -0.40 ± 0.50	1 ± 0/4 ± 2 -0.77 ± 0.47

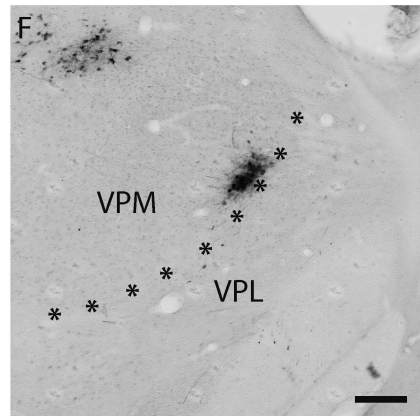
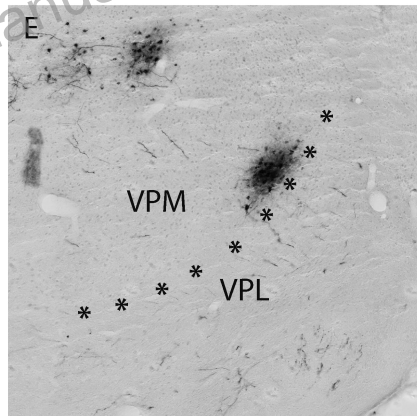
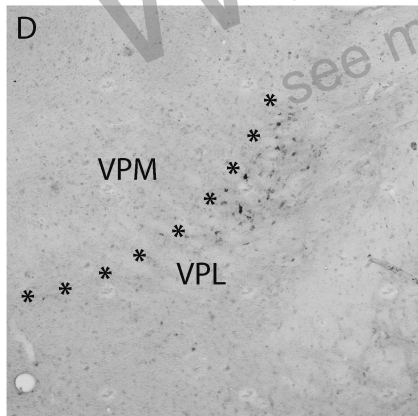
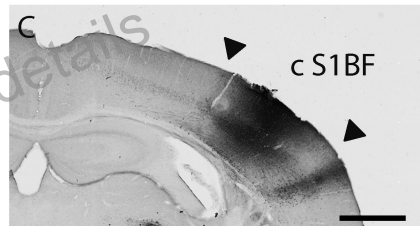
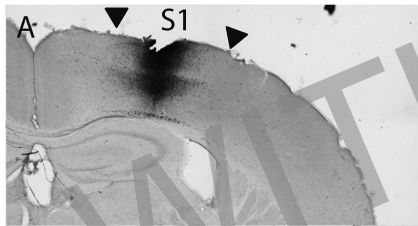
TABLE 6: Number and percentage (in parentheses) of retrogradely labeled neurons in sensory and non-sensory subcortical areas after injections of CTb into the primary somatosensory cortex (S1) of intact C57Bl/6 mice.

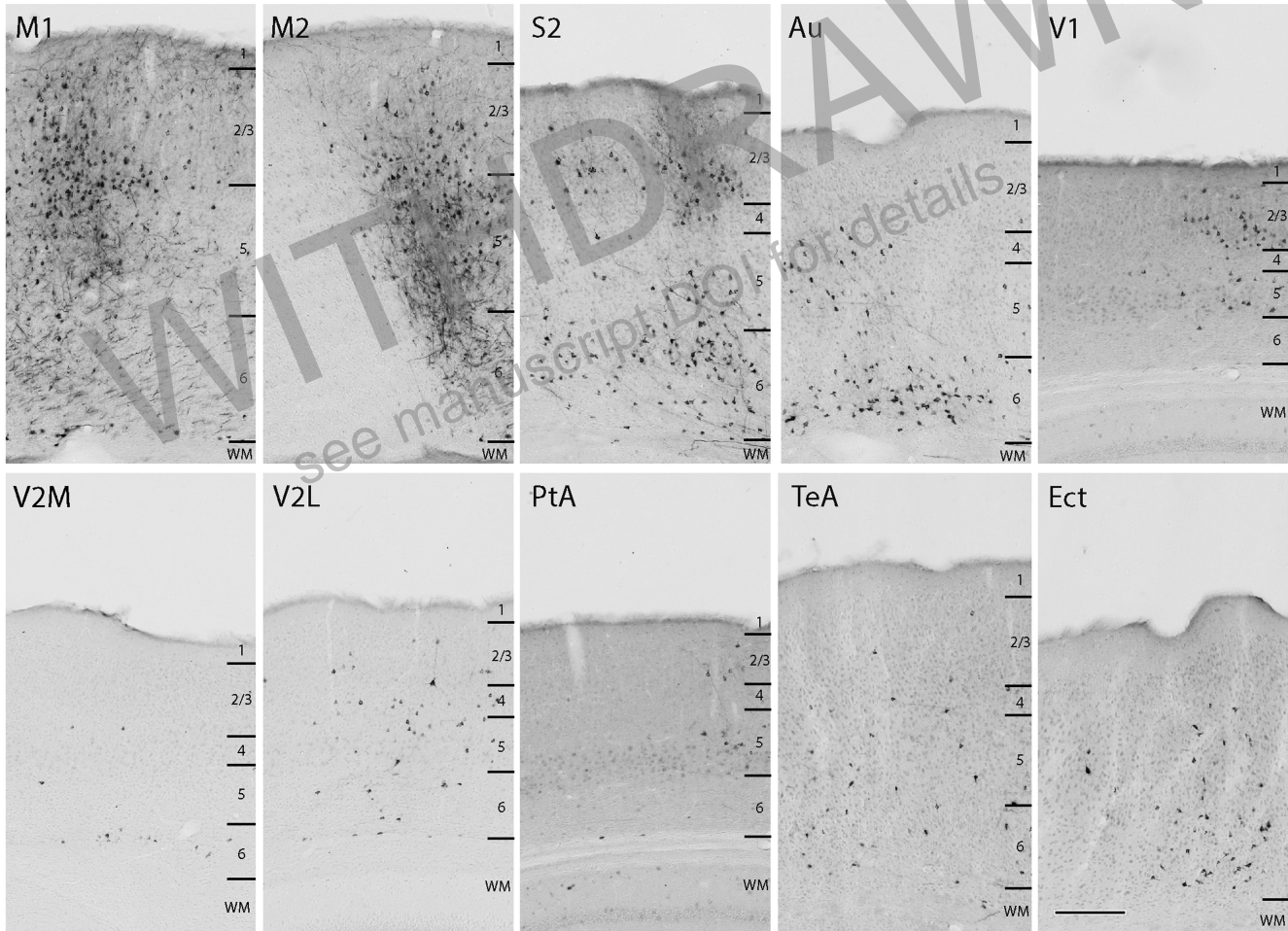
Injection site	Case	Subcortical area						
		Po	VPL	VPM	AM	VL	VM	Re
S1	02-03a4	64 (10.06)	510 (80.19)	0 (0)	0 (0)	0 (0)	0 (0)	0 (0)
	02-03a5	88 (12.61)	478 (68.48)	0 (0)	0 (0)	0 (0)	56 (8.02)	38 (5.44)
	02-03a3	70 (8.90)	502 (63.79)	0 (0)	0 (0)	0 (0)	85 (10.80)	43 (5.46)
	02-03a6	38 (8.56)	247 (55.63)	0 (0)	0 (0)	0 (0)	31 (6.98)	12 (2.70)
	02-03a7	123 (11.38)	729 (67.44)	0 (0)	0 (0)	0 (0)	68 (6.29)	38 (3.52)
	Mean ± SEM	76.60 ± 15.76 (10.30 ± 0.85)	493.20 ± 85.44 (67.11 ± 4.44)	0 ± 0 (0 ± 0)	0 ± 0 (0 ± 0)	0 ± 0 (0 ± 0)	48.00 ± 16.63 (6.42 ± 1.99)	26.20 ± 9.52 (3.43 ± 1.13)
r S1BF	03-02b2	294 (39.95)	0 (0)	258 (35.05)	0 (0)	0 (0)	8 (1.09)	0 (0)
	03-04a6	198 (30.18)	0 (0)	258 (39.33)	0 (0)	36 (5.49)	16 (2.44)	8 (1.22)
	03-04a7	434 (48.22)	0 (0)	162 (18)	0 (0)	68 (7.56)	114 (12.67)	48 (5.33)
	03-04b4	402 (31.31)	0 (0)	258 (20.09)	26 (2.03)	258 (20.09)	34 (2.65)	4 (0.31)
	03-04b5	376 (38.76)	0 (0)	226 (23.30)	8 (0.83)	108 (11.13)	52 (5.36)	18 (1.86)
	Mean ± SEM	340.80 ± 47.60 (37.68 ± 3.66)	0 ± 0 (0 ± 0)	232.40 ± 20.86 (27.16 ± 4.74)	6.80 ± 5.64 (0.57 ± 0.44)	94.00 ± 49.98 (8.85 ± 3.73)	44.80 ± 21.13 (4.84 ± 2.32)	15.60 ± 9.65 (1.74 ± 1.07)
c S1BF	03-02b7	263 (50.19)	0 (0)	165 (31.49)	10 (1.91)	19 (3.63)	3 (0.57)	2 (0.38)
	04-01b2	264 (36.72)	0 (0)	232 (32.27)	0 (0)	26 (3.62)	112 (15.58)	0 (0)
	03-02b4	580 (37.69)	0 (0)	111 (7.21)	12 (0.78)	59 (3.83)	61 (3.96)	16 (1.04)
	03-02b5	362 (30.17)	0 (0)	357 (29.75)	44 (3.67)	162 (13.5)	1 (0.08)	23 (1.92)
	03-02b6	215 (38.19)	0 (0)	200 (35.52)	11 (1.95)	48 (8.53)	2 (0.36)	6 (1.07)
	Mean ± SEM	336.80 ± 73.04 (38.59 ± 3.62)	0 ± 0 (0 ± 0)	15.40 ± 46.08 (27.25 ± 5.70)	15.40 ± 8.35 (1.66 ± 0.69)	62.80 ± 28.88 (6.62 ± 2.19)	35.80 ± 24.84 (4.11 ± 3.30)	9.40 ± 4.89 (0.88 ± 0.37)

Injection site	Case	Subcortical area						
		GP	PT	AHA	ZI	CM-PC	Hyp	CPu
S1	02-03a4	0 (0)	0 (0)	0 (0)	62 (9.75)	0 (0)	0 (0)	0 (0)
	02-03a5	0 (0)	0 (0)	0 (0)	26 (3.73)	2 (0.29)	2 (0.29)	0 (0)
	02-03a3	0 (0)	0 (0)	0 (0)	54 (6.86)	18 (2.29)	11 (1.40)	0 (0)
	02-03a6	0 (0)	0 (0)	0 (0)	22 (4.96)	87 (19.60)	5 (1.13)	0 (0)
	02-03a7	0 (0)	0 (0)	0 (0)	54 (5.00)	54 (5.00)	9 (0.83)	0 (0)
	Mean ± SEM	0 ± 0 (0 ± 0)	0 ± 0 (0 ± 0)	0 ± 0 (0 ± 0)	43.60 ± 9.12 (6.06 ± 1.17)	32.20 ± 18.76 (5.43 ± 4.08)	5.40 ± 2.31 (0.73 ± 0.29)	0 ± 0 (0 ± 0)
	r S1BF	03-02b2	28 (3.80)	0 (0)	0 (0)	22 (2.99)	108 (14.67)	16 (2.17)
	03-04a6	18 (2.74)	0 (0)	0 (0)	0 (0)	112 (17.07)	6 (0.92)	2 (0.31)
	03-04a7	8 (0.89)	0 (0)	0 (0)	2 (0.22)	34 (3.78)	20 (2.22)	10 (1.11)
	03-04b4	38 (2.96)	0 (0)	0 (0)	66 (5.14)	172 (13.40)	8 (0.62)	2 (0.16)
	03-04b5	24 (2.47)	0 (0)	0 (0)	30 (3.09)	104 (10.72)	14 (1.44)	4 (0.41)
	Mean ± SEM	23.20 ± 5.60 (2.57 ± 0.53)	0 ± 0 (0 ± 0)	0 ± 0 (0 ± 0)	24.00 ± 13.38 (2.29 ± 1.08)	106.00 ± 24.48 (11.93 ± 2.55)	12.80 ± 2.88 (1.48 ± 0.36)	3.60 ± 1.92 (0.40 ± 0.21)
c S1BF	03-02b7	16 (3.05)	1 (0.19)	2 (0.38)	6 (1.15)	24 (4.58)	13 (2.48)	0 (0)
	04-01b2	29 (4.03)	0 (0)	0 (0)	19 (2.64)	7 (0.97)	29 (4.03)	1 (0.14)
	03-02b4	25 (1.62)	0 (0)	0 (0)	38 (2.47)	143 (9.29)	49 (3.18)	61 (3.96)
	03-02b5	15 (1.25)	0 (0)	0 (0)	51 (4.25)	26 (2.17)	25 (2.08)	0 (0)
	03-02b6	17 (3.02)	0 (0)	0 (0)	15 (2.66)	24 (4.26)	10 (1.78)	0 (0)
	Mean ± SEM	20.40 ± 3.12 (2.60 ± 0.57)	0.20 ± 0.22 (0.04 ± 0.04)	0.40 ± 0.45 (0.08 ± 0.09)	25.80 ± 9.15 (2.63 ± 0.55)	44.80 ± 27.72 (4.26 ± 1.59)	25.20 ± 7.75 (2.71 ± 0.45)	12.40 ± 13.59 (0.82 ± 0.88)

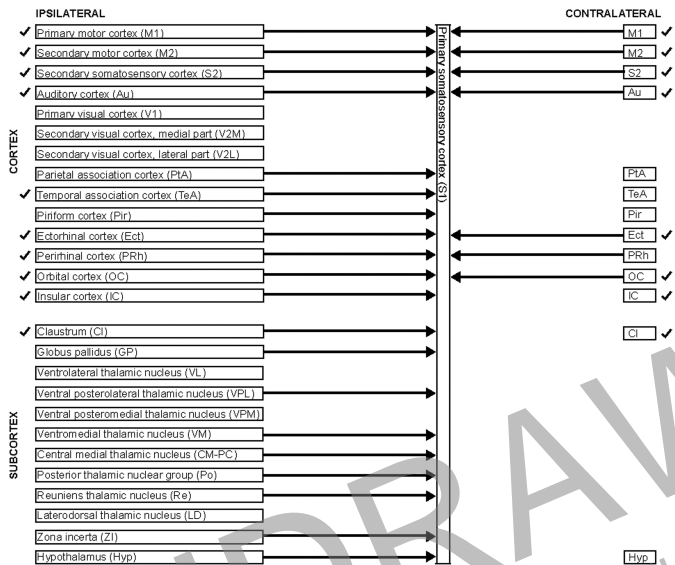
Injection site	Case	Subcortical area						
		LH	PVP	APTD	PM	mfb	VA	LSI
S1	02-03a4	0 (0)	0 (0)	0 (0)	0 (0)	0 (0)	0 (0)	0 (0)
	02-03a5	0 (0)	0 (0)	0 (0)	0 (0)	8 (1.15)	0 (0)	0 (0)
	02-03a3	0 (0)	0 (0)	0 (0)	0 (0)	4 (0.51)	0 (0)	0 (0)
	02-03a6	0 (0)	0 (0)	0 (0)	0 (0)	2 (0.45)	0 (0)	0 (0)
	02-03a7	0 (0)	0 (0)	0 (0)	0 (0)	6 (0.56)	0 (0)	0 (0)
	Mean ± SEM	0 ± 0 (0 ± 0)	0 ± 0 (0 ± 0)	0 ± 0 (0 ± 0)	0 ± 0 (0 ± 0)	4.00 ± 1.58 (0.53 ± 0.20)	0 ± 0 (0 ± 0)	0 ± 0 (0 ± 0)
	r S1BF	03-02b2	0 (0)	0 (0)	0 (0)	0 (0)	2 (0.27)	0 (0)
	03-04a6	0 (0)	0 (0)	0 (0)	0 (0)	2 (0.31)	0 (0)	0 (0)
	03-04a7	0 (0)	0 (0)	0 (0)	0 (0)	0 (0)	0 (0)	2 (0.22)
	03-04b4	0 (0)	0 (0)	0 (0)	0 (0)	0 (0)	0 (0)	0 (0)
	03-04b5	0 (0)	0 (0)	0 (0)	0 (0)	0 (0)	0 (0)	2 (0.21)
	Mean ± SEM	0 ± 0 (0 ± 0)	0 ± 0 (0 ± 0)	0 ± 0 (0 ± 0)	0 ± 0 (0 ± 0)	0.80 ± 0.55 (0.12 ± 0.08)	0 ± 0 (0 ± 0)	1.20 ± 0.55 (0.04 ± 0.04)
c S1BF	03-02b7	0 (0)	0 (0)	0 (0)	0 (0)	0 (0)	0 (0)	0 (0)
	04-01b2	0 (0)	0 (0)	0 (0)	0 (0)	0 (0)	0 (0)	0 (0)
	03-02b4	3 (0.20)	10 (0.65)	32 (2.08)	7 (0.46)	0 (0)	0 (0)	0 (0)
	03-02b5	0 (0)	0 (0)	0 (0)	0 (0)	11 (0.92)	0 (0)	0 (0)
	03-02b6	0 (0)	0 (0)	0 (0)	0 (0)	5 (0.89)	7 (1.24)	0 (0)
	Mean ± SEM	0.60 ± 0.67 (0.04 ± 0.04)	2.00 ± 2.24 (0.13 ± 0.15)	6.40 ± 7.16 (0.42 ± 0.47)	1.40 ± 1.57 (0.09 ± 0.10)	3.20 ± 2.43 (0.36 ± 0.25)	1.40 ± 1.57 (0.25 ± 0.28)	0 ± 0 (0 ± 0)

Injection site	Case	Subcortical area			
		STLP	AV	EP	VP
S1	02-03a4	0 (0)	0 (0)	0 (0)	0 (0)
	02-03a5	0 (0)	0 (0)	0 (0)	0 (0)
	02-03a3	0 (0)	0 (0)	0 (0)	0 (0)
	02-03a6	0 (0)	0 (0)	0 (0)	0 (0)
	02-03a7	0 (0)	0 (0)	0 (0)	0 (0)
	Mean ± SEM	0 ± 0 (0 ± 0)	0 ± 0 (0 ± 0)	0 ± 0 (0 ± 0)	0 ± 0 (0 ± 0)
	r S1BF	03-02b2	0 (0)	0 (0)	0 (0)
	03-04a6	0 (0)	0 (0)	2 (0.31)	0 (0)
	03-04a7	2 (0.22)	2 (0.22)	2 (0.22)	0 (0)
	03-04b4	0 (0)	4 (0.31)	0 (0)	4 (0.31)
	03-04b5	0 (0)	0 (0)	0 (0)	2 (0.21)
	Mean ± SEM	0.40 ± 0.45 (0.04 ± 0.04)	1.60 ± 0.84 (0.07 ± 0.07)	0.80 ± 0.55 (0.03 ± 0.03)	1.20 ± 0.89 (0.04 ± 0.04)
c S1BF	03-02b7	0 (0)	0 (0)	0 (0)	0 (0)
	04-01b2	0 (0)	0 (0)	0 (0)	0 (0)
	03-02b4	0 (0)	0 (0)	0 (0)	0 (0)
	03-02b5	0 (0)	0 (0)	0 (0)	0 (0)
	03-02b6	0 (0)	0 (0)	0 (0)	0 (0)
	Mean ± SEM	0 ± 0 (0 ± 0)	0 ± 0 (0 ± 0)	0 ± 0 (0 ± 0)	0 ± 0 (0 ± 0)

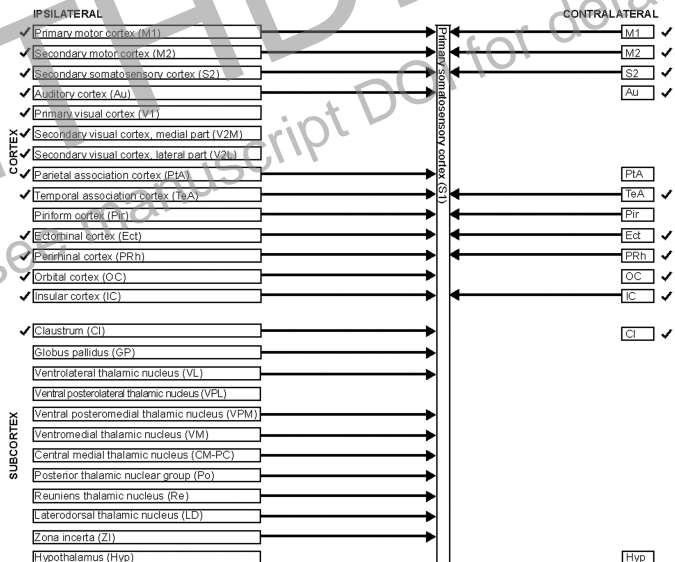




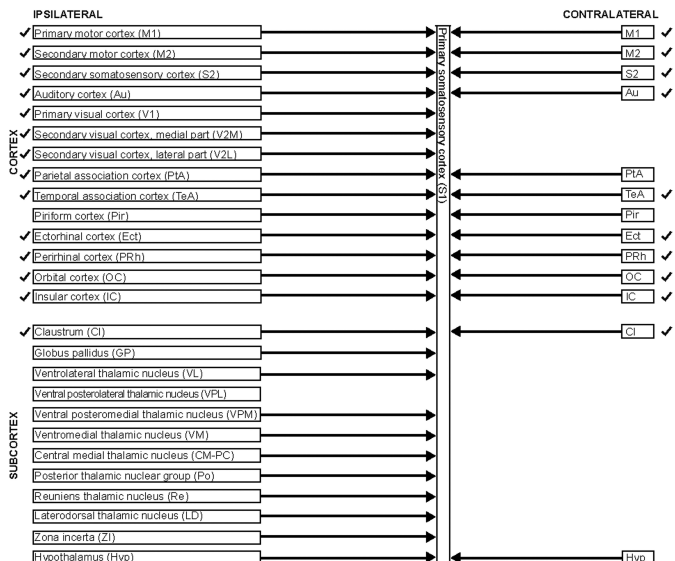
S1



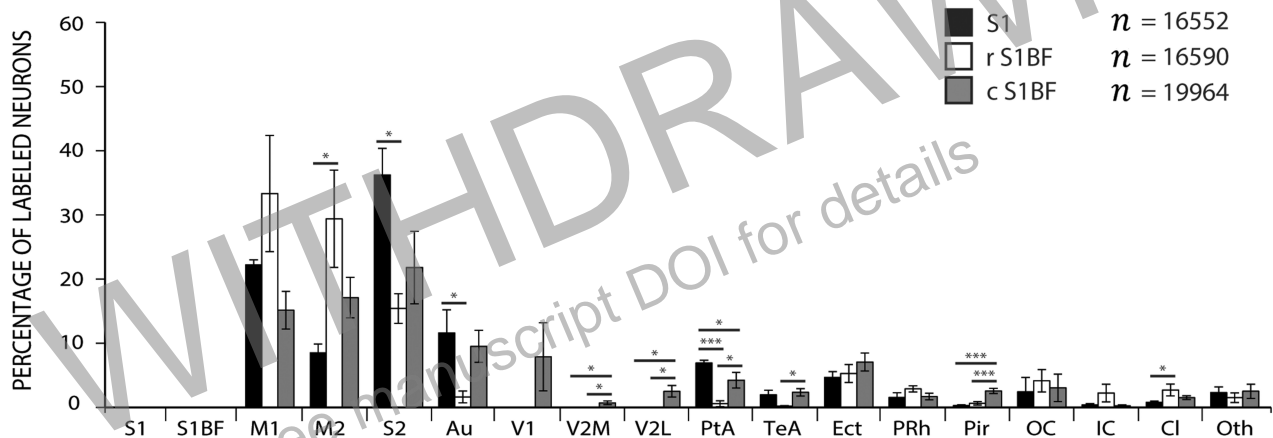
r S1BF



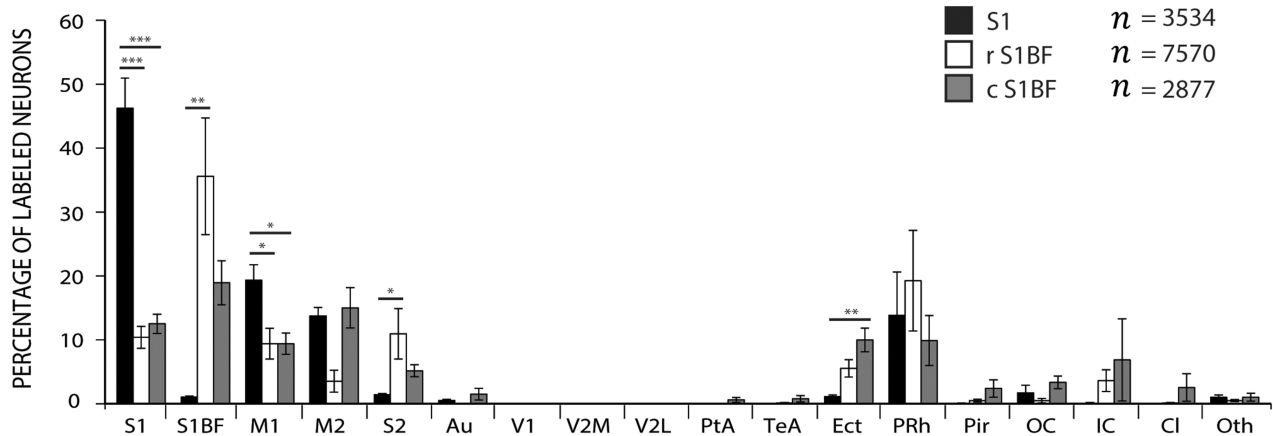
c S1BF

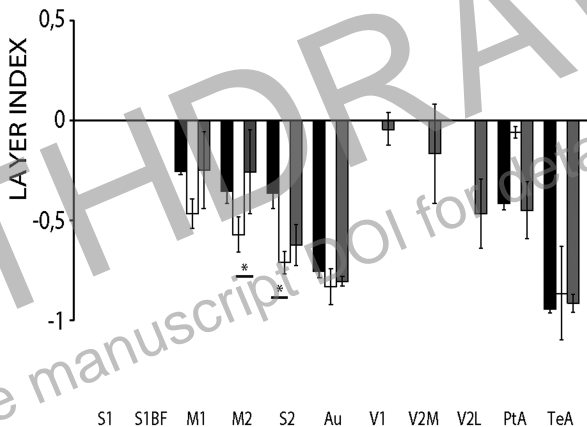


A



B



A**B**